11

2D Materials with 1D Semiconducting Nanostructures for High-Performance Gas Sensor

Shulin Yang[1,2], Yinghong Liu[1], Gui Lei[1,2], Huoxi Xu[1], Zhigao Lan[1], Zhao Wang[2], and Haoshuang Gu[1,2]

[1] *Huanggang Normal University, Hubei Key Laboratory for Processing and Application of Catalytic Materials, School of Physics and Electronic Information, 146 Xingang 2nd Road, Huanggang, Hubei Province, 438000, China*
[2] *Hubei University, Hubei Key Laboratory of Ferro & Piezoelectric Materials and Devices, Faculty of Physics and Electronic Sciences, 368 Youyi Road, Wuhan, Hubei Province, 430062, China*

11.1 Introduction

Gaseous pollution has been becoming a serious issue in modern society with the rapid development of industry and the increasing popularity of automobiles [1–3]. The high-concentration gas in the air poses serious threats to our health and our security in life [4–6]. It is reported that the colorless/toxic CO would interact strongly with the hemoglobin in our blood and prevent the red blood cells from transferring oxygen in our body, resulting in asthma, cardiovascular disease or cardiac disease, and even death with its concentration being over 5000 ppm [7]. Moreover, there would be a high risk of explosion when the CO concentration reaches 12.5–74.2% in the air [8]. The colorless, odorless, and tasteless H_2 could also cause an explosion with its concentration being in the range of 4–75.6% [9]. The greenhouse gases of CO_2 and CH_4 have been proved to be mainly responsible for global warming, resulting in serious changes in the climate [10]. And the SO_2 or NO_2 is also reported to be a threat gas to cause acid rain and would damage our health with the concentration being extremely low (ppm level) [11–13]. Additionally, the formaldehyde in modern decorative materials and the triethylamine (TEA) released with the decay of fishes and other seafood are potential threat gases, and they are also a danger to our health [14]. Therefore, high-performance gas sensors are of great importance and urgent demand to effectively detect or monitor the gases.

Recently, the one-dimensional (1D) semiconducting nanostructures have been more and more popular sensing materials to show promising sensing properties with their advantages of high surface activity, facile synthesization, small size,

1D Semiconducting Hybrid Nanostructures: Synthesis and Applications in Gas Sensing and Optoelectronics, First Edition. Edited by Arvind Kumar, Dinesh K. Aswal, and Nirav Joshi.

low cost, and good stability [15, 16]. Moreover, the 1D structure could be channels for the transport of carriers in the sensing material [17, 18]. Metal oxide-based gas sensors have attracted lots of attention, since the gas-sensing performance of the ZnO film was reported by Taguchi et al. in 1962 [19]. There are numerous metal oxides assembled to be the gas sensors, including TiO_2, Nb_2O_5, WO_3, In_2O_3, NiO, MoO_3, Fe_2O_3, or SnO_2 [16, 18, 20–26]. The sensor based on the single SnO_2 nanowire with a length of over 3 μm was reported to exhibit a sensor response (R_{air}/R_{gas}, R_{air} or R_{gas} presenting the resistance of sensor in air or target gas, respectively) of 6.76 50 ppm ethanol at the working temperature of 350 °C [27]. The work of Liu et al. suggested that the electrospun In_2O_3 nanowires could be a possible sensing material to detect 1 ppm acetone under 100% RH at 320 °C with the response/recovery time being 11/13 seconds [28]. And the NiO nanowires with average length and diameter being ~20 μm and ~120 nm, respectively, yield a sensor response (R_{air}/R_{gas}) being ~13–100 ppm formaldehyde at 200 °C [29]. Meanwhile, the sensor based on the decorated Si nanowires was found to be a potential substrate to sense 1 mbar CO_2 with the response time or recovery time being 95 or 103 seconds, respectively [30]. Based on these reports, it was reasonable to infer that the sensors based on the pure semiconducting nanostructures could be used to detect various gases but with the relatively low sensor responses or long response/recovery times, a negative factor constraining the promotion of their application in the gas sensor.

The construction of heterojunction is proved to effectively improve the gas-sensing performances of 1D semiconducting nanostructures [20, 31]. The two-dimensional (2D) materials have been also widely used to composite with the 1D metal oxides to assemble high-performance gas sensors with their advantages of high specific surface area and unique chemical and physical properties [32–34]. As it was reported, the gas-sensing performance of metal oxide was mainly attributed to the redox reaction between the chemisorbed oxygen species and the target gas molecules [20, 35]. The sheet-like structure and the abundant active site of the 2D materials would fascinate the adsorptions and diffusions of gas molecules in the composite. The sensor response of the ZnO nanorods composited with reduced graphene oxide (RGO) was reported to be ~70% ($\Delta R/R_{gas}$*100%, $\Delta R = R_{air} - R_{gas}$) toward 400 ppb NO_2 at the working temperature of 22.4 ± 0.2 °C [36]. The formaldehyde sensing performance of the SnO_2 nanowires was also improved with decorating with RGO, exhibiting a higher sensor response (R_{air}/R_{gas}) of 5437 to 50 ppm formaldehyde at 50 °C [37]. The investigation of Xu et al. showed that the sensor response (R_{air}/R_{gas}) of the ZnO nanorods toward 100 ppm ethanol at 350 °C was effectively enhanced from the original 15 to 125 via compositing them with sheet-like Co_3O_4 nanostructures [38]. Nowadays, both the typical 2D materials of the graphene or RGO, MoS_2, or WS_2 and the synthesized sheet-like NiO, ZnO, or SnO_2 have been applied to enhance the sensing response of the metal oxides with the establishment of heterojunctions. The sensor response of the composite was higher than that of the pure metal oxide, and the working temperature could also be decreased at the same time. Some reviews have compared the gas-sensing performances of the 1D metal oxides and reported their gas-sensing mechanisms [20, 21, 31, 35].

However, there were few reports focusing on the gas-sensing properties of the 1D semiconducting nanostructures composited with 2D materials.

In this work, we have compared the sensing performances of the sensors based on 1D semiconducting nanostructures composited with 2D materials and discussed their assembly process. We have discussed the gas-sensing properties of the 1D-sensing materials decorating with graphene/RGO, MoS_2, WS_2, NiO nanosheet, ZnO nanosheet, or the other 2D materials. The method to construct the 1D nanomaterial of a nanowire, nanorod, nanoribbon, or nanofiber composited with 2D sheet-like material is discussed and summarized. The sensor response, the response time, and the recovery time are compared in detail, and the improved sensing mechanisms are discussed as well. Additionally, the potential challenges and the possible methods to further improve the sensing based on 2D materials with 1D semiconducting nanostructures are proposed.

11.2 Enhanced Gas-Sensing Performances of 1D-Sensing Materials Composited with Different 2D Materials

The 2D materials have been widely applied to decorate with metal oxides to improve their gas-sensing performances. And a series of methods could be successfully to construct the heterostructure of 2D materials with 1D semiconducting nanostructures, mainly a two-step process. The introduction of 2D material could effectively increase the special surface area and provide more active sites in the composite, a positive factor for improving the gas-sensing response of 1D semiconducting materials. Some of the common 2D materials were reviewed in this study, mainly including graphene-based material, MoS_2, WS_2, NiO, or ZnO.

11.2.1 Graphene or Reduced Graphene Oxide-based Composites

The graphene has attracted lots of attention since it was first synthesized and reported in 2004 [39]. The graphene and the graphene-based materials are widely applied in gas sensors due to their unique layer structures and the special physical/chemical prosperities [40]. The graphene oxide (GO) is one of the typical graphene-based materials and has been popularly used to decorate the metal oxides to enhance their gas-sensing performance with the abundant functions groups on their surfaces [41, 42]. In some work, the RGO was also directly described as graphene because a majority of the functional groups were removed from the surface of the GO during the synthesization of the composite. In this review, the GO-based sheet in the final composite has been uniformly described as RGO.

Roshan et al. suggested that the graphene-decorated ZnO nanowires were reported to be a potential substrate to sense ethanol [43]. The authors firstly prepared a mixture of zinc acetate and 2-methoxyethanol and then further added the monoethanolamine into the obtained mixture to obtain the seed solution. The seed solution was spin-coated on the surface of the electrode covered with a layer

of graphene. The scanning electron microscopy (SEM) image of the used graphene was shown in Figure 11.1a,b. The treated electrode was immersed into a precursor of $Zn(NO_3)_2$ and hexamethylenetetramine. The ZnO nanowires were directly grown on the surface of the graphene covered on the electrode through a hydrothermal method at 70 °C (seen the inset in Figure 11.1f). The average length of the prepared hexagonal ZnO nanowires was ~2 μm with the average diameter being 100–200 nm (Figure 11.1c–e). The sensor based on the graphene-decorated ZnO nanowires exhibited a senor response (R_{air}/R_{gas}) of ~23 at the optimal working temperature of 125 °C, over five times higher than that of the pure ZnO nanowires (~3.5) at a higher working temperature of 200 °C (Figure 11.1f–h). The authors also pointed out that the pure ZnO nanowires exhibited a typical n-type sensing performance to ethanol, while a p-type sensing property of graphene-decorated ZnO nanowires was observed. The sensor response of the decorated ZnO nanowires to 1–50 ppm ethanol was higher than that of the pure ones. And the graphene-decorated ZnO nanowires also presented a higher sensor response to 20 ppm ethanol at 125 °C compared with that to 1000 ppm CH_4, 100 ppm CO, 4000 ppm H_2O, 1000 ppm CO_2, or 1000 ppm CH_2O (Figure 11.1i), indicating the good selectivity of the composite. The different work functions of the ZnO (~4.45 eV) and the graphene (4.9 eV) would result in the bending of their bands and form a potential barrier at the heterojunctions. When the ethanol was introduced on the surface of the sensing material, the released electrons could effectively decrease the height of the potential barrier, leading to a higher sensor response of the composite. On the other hand, the electrons would mainly be transferred through the graphene due to its high mobility and high conductivity, facilitating the transport of carries in the sensing material during the sensing performance. Then, an enhanced sensing performance of the composite was achieved due to the decoration of graphene acting as a high conductive carrier path. This research indicated that the sensing performance of the metal oxide could be improved with the help of graphene. It should be noted that there were only some references reporting the metal oxides decorated with pure graphene. We found that more attention was focused on improving the gas-sensing performances of metal oxides composited with RGO.

The work of Lee's team reported that the sensing performance of vertical zinc oxide nanorods was enhanced through compositing them with RGO [44]. The authors have directly assembled the RGO-decorated ZnO on the surface of AlGaN/GaN layer. The ZnO nanorods array was grown on a prepared substrate without a seed layer at 90 °C for 4 hours. A modified Hummers' method was applied to synthesize the RGO with an average thickness or size of ~3 or ~200 nm, respectively. Then the prepared RGO was adsorbed on the ZnO nanorods modified with poly(diallydimethylammonium chloride) (PDDA) via a drop-casting method, and the assembled sensor was further annealed at 120 °C for three hours to enhance its stability. The sensor based on the composite showed promising sensing properties to NO_2, SO_2, or HCHO gas with low concentrations of 120–1000 ppb. The composite showed a typical p-type sensing performance toward NO_2 or SO_2 but an n-type sensing response to HCHO. The composite exhibited a sensor response ($\Delta R/R_{air}$, $\Delta R = R_{air} - R_{gas}$) of 1.875 ppm^{-1} toward 120 ppb NO_2 with the response/recovery

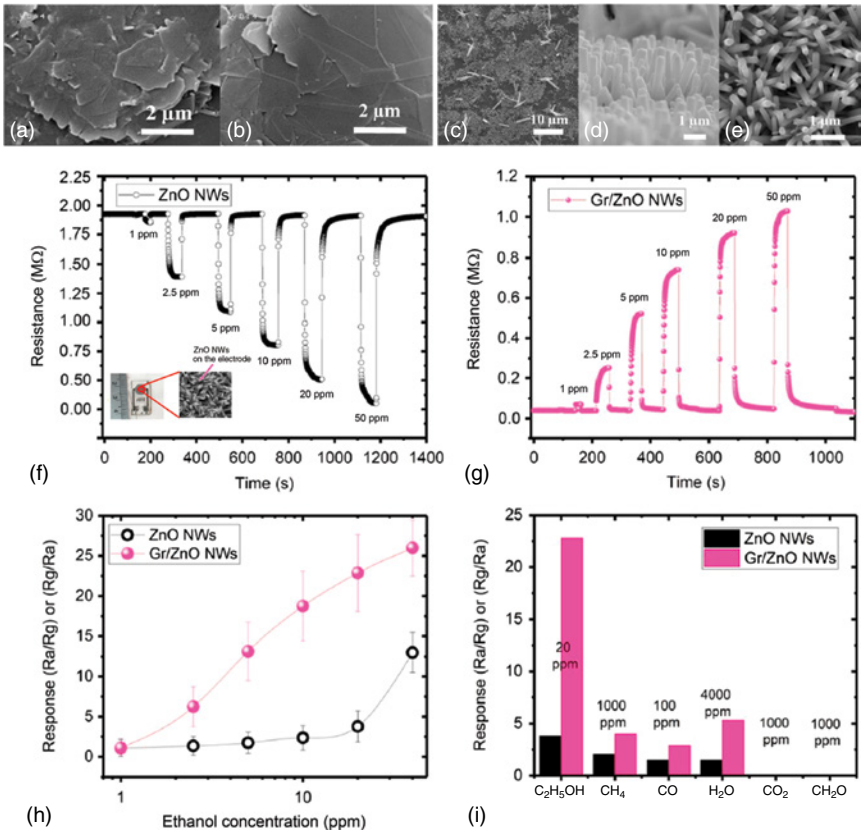

Figure 11.1 SEM images of graphene (a and b) and ZnO nanowires composited with graphene nanowires. (f–h) The gas-sensing performances of pure ZnO nanowires and ones composited with graphene nanowires, the inset in (f) is the digital image of the assembled sensor and the SEM image of the ZnO nanowires on the electrodes. (i) The gas selectivity of ZnO nanowires and the composite toward different gases. Source: Rafiee et al. [43], Reproduced with permission from Elsevier.

time being 120/320 seconds at room temperature (300 ± 1 K). The sensor response of the composite to NO_2 was higher than that to SO_2 ($0.933\,ppm^{-1}$) or HCHO ($0.875\,ppm^{-1}$). This research paved a possible way to design the effective sensing material to show high-sensitive gas-sensing performance with low power consumption, and functionality at a low working temperature. According to the reported results, the sensor based on the RGO-decorated ZnO on AlGaN/GaN layer could be an effective material to detect hazardous gas with a low detection limit. It might be better if the sensing selectivity of the sensor to different gas was improved because the sensor showed a relatively high and close sensor response to NO_2, SO_2, or HCHO gas. And the shift of the baseline of the assembled sensor was also found during the sensing response, which should also be improved to ensure the accuracy and the sensing stability of the composite.

Gu et al. have assembled a sensor based on the MoO_3 nanoribbons decorated with RGOs (directly described as graphene in the work) and studied their hydrogen-sensing performance [45]. The GOs were prepared with a similar modified Hummers' method and then added into the precursor to construct the MoO_3 nanoribbons/RGO composite via a hydrothermal method. The average length of the MoO_3 was ~10 μm, and the RGO also remained the sheet-like morphology (Figure 11.2a–d). The MoO_3 composited with the 1.5 wt% RGO exhibited optimal hydrogen-sensing performance with the senor response (R_{air}/R_{gas}) being 8.83–500 ppm H_2 in the air at room temperature, as shown in Figure 11.2e,f. The sensor also could be used to effectively detect hydrogen gas with the concentration being 0.5–1000 ppm at room temperature (Figure 11.2g). And the senor based on composited exhibited a high senor response of ~20.5, one time higher than that of the pure MoO_3, with the response/recovery time being ~10/30 section (Figure 11.2h). The higher specific surface area, the formation of heterojunction around the interfaces, and the improved electronic conductivity were reported to be mainly responsible for the enhancement hydrogen gas-sensing performance of the MoO_3 nanoribbons/RGO composite. The remarkable hydrogen selectivity and repeatability were also reported by the authors, further indicating the potential of the composite in the area of the hydrogen gas sensor.

Kim et al. have assembled a sensor based on the ZnO nanofibers decorated with RGO nanosheets and studied their potential application in hydrogen sensors [46]. The GO was firstly prepared with a modified Hummers' method, and then the RGO was obtained by an oil bath with the hydrazine monohydrate. The solution of the prepared RGO and the zinc acetate was used to synthesize the RGO-decorated ZnO nanofibers through an electrospinning method, and then the prepared composite was annealed at 600 °C in the air for 30 minutes. The RGO-decorated ZnO nanofibers exhibited an optimal sensor response of 2524 (R_{air}/R_{gas}) to 10 ppm H_2 at the optimal working temperature of 400 °C. Moreover, the composite also exhibited a promising sensor response of 866 to 0.1 ppm H_2 at 400 °C with the response time or recovery time being 3.5 or 3.9 minutes, respectively. The authors also compared the hydrogen-sensing performance of the RGO-loaded ZnO nanofibers with that of the RGO-loaded SnO_2 nanofibers. The sensor response of the former composite to 10 ppm H_2 at 400 °C was approximately 25 times higher than that of the latter one (74.8), inferring the more superior hydrogen-sensing performance of the RGO-loaded ZnO nanofibers. In the H_2 atmosphere, there would be a metallic Zn layer along the junctions between the RGO and the ZnO nanofibers, making the ZnO more n-type. And the released electrons would not be transferred from the ZnO to the RGO during the sensing process, further improving the conductivity of the ZnO and resulting in a lower resistance of the composite. The spillover effect of the RGO would also enhance the sensing response of the RGO-loaded ZnO nanofibers. These three factors should be mainly responsible for the excellent hydrogen-sensing performance of the RGO-loaded ZnO nanofibers. Even the working temperature was relatively high, the excellent senor response (865.9) of the composite to H_2 with a low concentration of 0.1 ppm also indicated its great potential in the application of hydrogen gas sensors. This work also provided a possible way to construct the

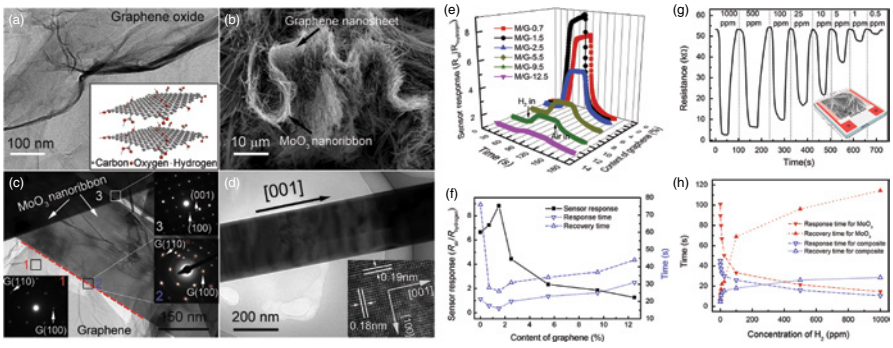

Figure 11.2 SEM image of graphene oxide (a) and the MoO_3 nanoribbons composited with RGO (b). (c) TEM image and the selected area diffraction (SAED) patterns of RGO and MoO_3 nanoribbon in the composite. (d) TEM image of single MoO_3 nanoribbon. (e and f) Hydrogen-sensing performance of composite with different content of RGO. (g and h) Dynamic sensing performance of the composite to 0.5–1000 ppm H_2 at room temperature, the inset in (g) is the sketch of the assembled gas sensor. Source: Yang et al. [45], Reproduced with permission from Elsevier.

promising sensing material to exhibit a high and stable sensor response to low-concentration hydrogen gas.

The RGO-decorated In_2O_3 nanofibers, reported by Gao et al., were found to show improved NO_2-sensing performance at a low working temperature of 50 °C [47]. The In_2O_3 nanofibers decorated with RGO nanosheets were synthesized via a similar process proposed by Kim et al. discussed ahead. In the work of decorated In_2O_3 nanofibers, the GO was also firstly prepared through a modified Hummers' method at a high temperature of 500 °C for two hours. The obtained GO was added into the precursor with raw materials of $In(NO_3)_3{\cdot}4.5H_2O$ and DMF solution to synthesize the decorated In_2O_3 nanofibers. The effects of the concentration of RGO on the NO_2-sensing performance of the In_2O_3 were studied via adding different contents of GO. The results showed that the sensor response (R_{gas}/R_{air}) of the decorated In_2O_3 nanofibers was 20.0, 42.0, and 26.6 to 5 ppm NO_2 at 50 °C for the composites with 1.1 wt%, 2.2 wt%, and 3.6 wt% RGO, respectively. Then the sensor based on the 2.2 wt% RGO-In_2O_3 nanofibers showed optimal NO_2-sensing performance among all the samples. Meanwhile, the sensor response of the composite was approximately 4.4 times higher compared with that of the pure In_2O_3 (9.5). In addition, further research showed that the 2.2 wt% RGO-In_2O_3 nanofibers exhibited a promising sensor response of 1.8 or 10 to the NO_2 with the low concentration of 1 or 2 ppm, respectively. The response time and the recovery time of the optimal composite to 5 ppm NO_2 at 50 °C were 261 and 698 seconds, respectively, also shorter than those of the pure In_2O_3 (316 and 1669 seconds). The enhanced NO_2-sensing performance of the decorated In_2O_3 was reported to be ascribed to the modification of the resistance with the formation of p–n heterojunction between the RGO and the In_2O_3 and the high special surface area of the composite. The special surface area of the decorated In_2O_3 was calculated to be 315.30 m^2/g, approximately 10 times higher compared with pure In_2O_3. The rich defects and the dangling bonds in the RGO provide more adsorption sites for the NO_2 and fascinate the adsorptions of more NO_2, also resulting in the enhanced gas-sensing property of the composite. This research further revealed that the GO could be applied to synthesize RGO-decorated nanofibers via a two-step method to construct effective material with promising gas-sensing performance. It should also be noted that the humidity showed a significant effect on the gas-sensing performance. Both the sensor response and the resistance exhibited a negative relationship with the humidity, which might be a factor that constrains the practical application of the sensor based on RGO-decorated In_2O_3 nanofibers.

The research of Galstyan et al. revealed that the hydrogen-sensing performance of the TiO_2 nanotubes was highly improved via decorating them with RGO nanosheets [48]. The TiO_2 nanotubes were synthesized with a method of electrochemical anodization with the raw material of titanium films with the thickness of 500 nm which was deposited on the substrate of Al. Then the obtained tubular structures were annealed in the O_2/Ar atmosphere at 400 °C for six hours. The GO used in the study was prepared with a widely modified Hummers' method and then dropped on the surface of the obtained TiO_2 nanotubes arrays. Then the GO-decorated TiO_2 nanotubes were further annealed at 400 °C for four hours to reduce

the GO to be RGO. The authors have assembled a series of sensors based on TiO_2 nanotubes loaded by RGO with different contents. The results showed that the TiO_2 nanotubes with 4.5 ng/mm^2 GO exhibited a higher sensor response ($\Delta I/I_{air}$, $\Delta I = I_{air} - I_{gas}$, R_{air} or R_{gas} presenting the current of sensor in air or target gas, respectively) compared with that of the nanotubes composited with 0 ng/mm^2 GO or 40.5 ng/mm^2 GO. The sensor response of the RGO-decorated TiO_2 nanotubes was ~37.6 to 480 ppm H_2 at the working temperature of 200 °C. But the corresponding response time or recovery time was reported to be 1110 or ≤ 300 seconds, respectively, too long to meet the practical requirements of the hydrogen gas sensor.

Yang et al. suggested that the RGO-decorated ZnO nanowires could be used to detect NH_3 with promising sensing performance [49]. The ZnO nanowires were synthesized with a modified carbothermal reduction and the GO was prepared via a modified Hummers' method. The RGO-decorated ZnO nanowires were obtained by mixing the prepared ZnO nanowires and the collected GO, and then the mixture was annealed at 300 °C. The ZnO nanowires with an average length of 1.5 μm were well dispersed on both sides of the RGO. The electrodes were fabricated with a standard micro-electromechanical systems (MEMS) process, and the sensing material was deposited on the center zone of the obtained Au electrodes to assemble the gas sensor. Moreover, the authors also designed an operating system and peripheral circuits to assemble a portable gas-sensing device with five separated parts of power supplies, signal modulating circuits, analog-to-digital (A/D) conversion circuits, microprogrammed control unit (MCU), and hosting computer. The assembled sensor presented a good sensing performance to NH_3 with the concentration in the range of 500 ppb to 5000 ppm The sensor response showed a positive relationship with the concentration of NH_3. The sensor response ($\Delta R/R_{air}$*100%, $\Delta R = R_{gas} - R_{air}$) of the composite was 7.2% or 3% to 1 ppm or 500 ppb NH_3, respectively. The wire-like morphology of the ZnO in the composite could be channels for electrons transfer and provided more active sites for more O_2 molecules or NH_3, resulting in the enhancement of the NH_3-sensing performance of RGO-decorated ZnO.

Similar improvement was also reported in the study on gas-sensing performance of Cu_2O nanorods modified by RGO nanosheets, graphene–WO_3 composite, MoO_3–RGO hybrids, ultrathin ZnO nanorods–RGO mesoporous nanocomposites, ZnO nanowire–RGO nanocomposite, In_2O_3 nanorod-decorated RGO composite, RGO-decorated GaN nanorod or vanadium-doped cerium oxide nanorods wrapped RGO toward NH_3, acetaldehyde, H_2S, NO_2, NO_x, or H_2 [50–57].

11.2.2 MoS_2-based Composites

The MoS_2 is also one of the typical 2D materials and has attracted more and more attention in recent years, which was widely to decorate the metal oxides to improve their gas-sensing properties [58]. The ZnO nanorods decorated with MoS_2 nanosheets were reported to be successfully assembled via a typical two-step process. The array of the uniform ZnO nanorods with an average diameter of 100 nm was firstly prepared by immersing a patterned Si substrate covered with ZnO seeds in the nutrition solution consisting of zinc nitrate hexahydrate and

hexamethylenetetramine at 95 °C for seven hours (Figure 11.3a–d). The MoS_2 nanosheets were synthesized with the ultrasonication of MoS_2 powder in ethanol for 90 minutes and then collected by centrifugation. Then the obtained MoS_2 nanosheets were dropped on the surface of the ZnO nanorods and were further heated at 90 °C to prepare the MoS_2-decorated ZnO nanorods (Figure 11.3e–k). The assembled sensor was reported to be limited in a small size with a compact structure, as shown in Figure 11.3a. The sensor response ($\Delta R/R_{air}$*100%, $\Delta R = R_{gas} - R_{air}$) of the pure ZnO nanorods was calculated to be 184% toward NO_2 with the concentration being as low as 100 ppb. With the decoration of MoS_2 on ZnO, the sensor response was highly improved to be 1280% (Figure 11.3l,m), which was over seven times higher than that of the pure ZnO. The response time of the sensor to 200 ppb NO_2 was 118 seconds, and the recovery time of the sensor was short toward 500 ppb NO_2, being 32 seconds. Meanwhile, there was also a linear relationship between the sensor response and the concentration of NO_2 in the range of 5–100 ppb (Figure 11.3n). The outstanding NO_2-sensing performance of the composite was mainly attributed to the abundant adsorption sites in the composite and the fast charge carrier migration between the heterojunction. The lowest detection limit of the sensor based on the ZnO nanorods decorated with MoS_2 nanosheets was estimated to be as low as approximately 0.2 ppb. The lowest detection limit was so low that also revealed the advantages of the prepared composite. This investigation paves a possible way to improve the NO_2-sensing performance of the sensor based on metal oxides.

More recently, the SO_2-sensing performance of the SnO_2 nanofibers was also reported to be highly enhanced via decorating them with 2D MoS_2 nanosheets [59]. The MoS_2 nanosheets-decorated SnO_2 nanofibers were prepared through a two-step method that was similar to the way in ref. [58]. The uniform SnO_2 nanofibers were synthesized via one-chip electrospinning, and the MoS_2 nanosheets were prepared through a treatment of exfoliation of bulk MoS_2 with a high-power ultrasonic probe. The composite was then assembled by dropping the dispersed solution of the MoS_2 nanosheets on the surface of the SnO_2 nanofibers. The sensor based on the MoS_2 nanosheets-decorated SnO_2 nanofibers exhibited an enhanced SO_2-sensing performance at 150 °C with a sensor response (R_{gas}/R_{air}) being 10 times higher than that of the pure SnO_2 nanofibers. Meanwhile, the composite also could be operated at a lower working temperature (150 °C) compared with the pure SnO_2 nanofibers (300 °C). The authors pointed out that the decorated SnO_2 nanofibers were the potential to sense SO_2 with a low gas concentration of 1 ppm due to the high carrier mobility and low electrical noise of the MoS_2 nanosheets. This is a typical advantage of the senor based on the MoS_2 nanosheets-decorated SnO_2 nanofibers, making the composite be promisingly applied to detect SO_2 with outstanding performance. The chemical sensitization of MoS_2 nanosheets and the heterojunction between the MoS_2 and the SnO_2 were mainly responsible for the enhanced gas-sensing performance of the composite. We should note that the MoS_2 nanosheets were dispersed on the SnO_2 nanofibers, making the heterojunctions be formed via physical interaction between the MoS_2 and the SnO_2. Then the sensor response of the composite was not very high, being 11.1 to 10 ppm SO_2

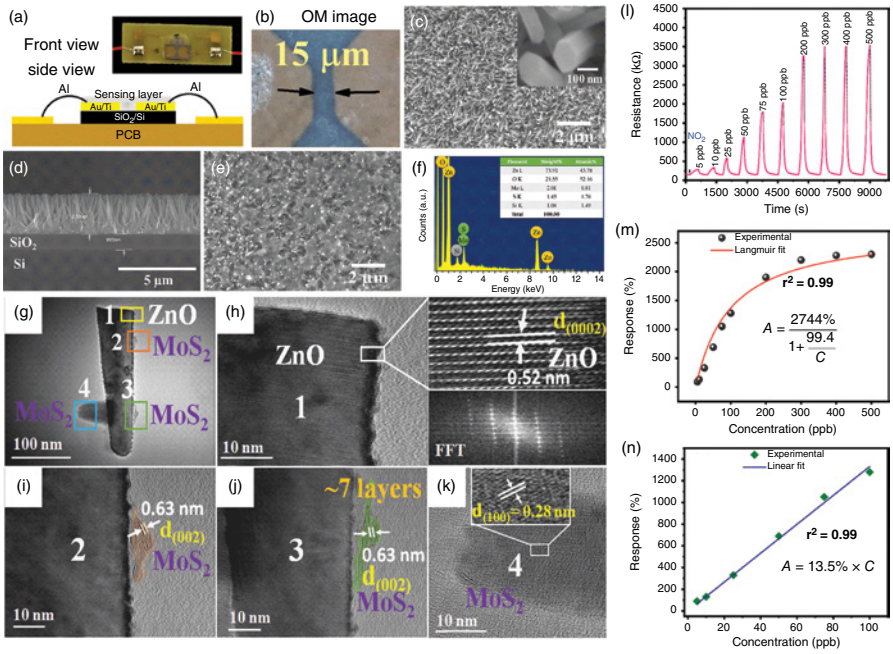

Figure 11.3 The sketch (a) and the optical micrograph image (b) of the assembled gas sensor. Low-resolution SEM image of top view (c) and the cross-sectional view of (d) the ZnO nanorods. (e) SEM image and (f) EDS spectrum of ZnO nanorods decorated with MoS_2 nanosheets. TEM image and the HRTEM image of the ZnO nanorods and the MoS_2 nanosheets in the composites (g–k). (l) Dynamic gas-sensing performance of the decorated ZnO nanorods to 5–500 ppb NO_2. (m and n) The relationship between the NO_2 concentration and the sensor response of the composite. Source: Kumar et al. [58], Reproduced with permission from Elsevier.

150 °C. If the MoS_2 nanosheets were directly synthesized on the surface of the SnO_2 nanofibers, the sensor based on the composite might exhibit a more promising sensing performance to SO_2 compared with the results reported by the authors.

The study of Lin et al. also revealed that the gas-sensing performance of the SnO_2 nanotubes could be enhanced through decorating them with MoS_2 nanosheet and polyaniline [60]. The SnO_2 nanotubes were synthesized through an electrospinning process with the working voltage being 21 kV followed by annealing at a high temperature of 500 °C in the air for two hours. The MoS_2 nanosheets were then decorated on the surface of the prepared SnO_2 nanotubes via a hydrothermal method with the raw materials of $(NH_4)_2MoS_4$ and $N_2H_4{\cdot}H_2O$ at 210 °C. An in situ polymerization was applied to construct the MoS_2 nanosheets/SnO_2 nanotubes decorated with polyaniline (PMS). The results showed the specific surface area of the PMS (49.2 m^2/g) was almost the same as that of the MoS_2 nanosheets/SnO_2 nanotubes, a positive factor facilitating the adsorption and the diffusion of the gas molecules reported by the authors. The NH_3-sensing performance of the MoS_2 nanosheets/SnO_2 nanotubes was found to be further enhanced with the decoration of polyaniline. The sensor response (R_{gas}/R_{air}) of the MoS_2 nanosheets/SnO_2 nanotubes was just slightly higher than 1–100 ppm NH_3 at ~24 °C. Then the sensor response of the PMD was effectively improved to be 10.9 with a short response/recovery time being 21/130 seconds. Moreover, the sensor based on the PMS exhibited promising sensing performance to 0.5–100 ppm NH_3 with the detection limit being as low as 200 ppb. It was reported that the high humidity always showed negative effects on the gas-sensing performance gas sensor based on metal oxide. Interestingly, the gas-sensing response of the prepared PMS was found to have a positive relationship with the humidity in the experiment. The sensor was reported to smoothly detect 50 ppm NH_3 under the humidity in the range of 20–80% with the sensor response increasing from ~5 under 20% RH to ~10 under 80% RH. This was possibly attributed to the reaction between the NH_3 and the water molecule and the greater deprotonation rate of the reaction product than NH_3 on the surface of the PMS. This work also revealed that the gas-sensing performance of the 1D material/2D material composite could be further enhanced with modification of the third-phase material, which would be applied to explore new gas-sensing materials with promising material for reference.

The study of Wang et al. also showed the SnO_2 nanotubes decorated with MoS_2 nanosheets exhibited outstanding NO_2-sensing performance at room temperature [61]. The authors also synthesized the SnO_2 nanotubes via a method of electrospinning with the raw material of $SnCl_2{\cdot}2H_2O$ and the constant voltage being 15 kV combined with an annealing treatment at 500 °C. And the MoS_2 nanosheets were vertically grown on the surface of the SnO_2 nanotubes through a hydrothermal method with the $C(NH_2)_2S$ and $Na_2MoO_4{\cdot}2H_2O$ at 200 °C for 12 hours. The resistance of the obtained SnO_2 nanotubes decorated with MoS_2 nanosheets decreased quickly when the NO_2 was injected, indicating the n-type sensing response of the obtained composite. The sensor response (R_{air}/R_{gas}) of the decorated SnO_2 nanotubes was found to be 34.67–100 ppm NO_2, ~26.5 times higher than that of the pure SnO_2. And the response time was also calculated to be as short as 2.2 seconds with

the recovery time being 10.54 seconds. The low detection limit of the SnO_2 nanotubes decorated with MoS_2 nanosheets was only 10 ppb, revealing the potential application in the area of hydrogen sensors. Additionally, the composite also showed excellent sensing repeatability and long-term stability to NO_2 with promising selectivity. The enhanced chemisorbed oxygen on the surface of the composite was reported to be one factor for the improvement in their NO_2 gas-sensing performance. The formation of p–n heterojunction further provided more active sites for the gas molecules and accelerated the charge transfer between the adsorbed gas molecules and the decorated SnO_2 nanotubes, another positive factor for the enhanced NO_2-sensing response. This research further inferred that the 2D MoS_2 nanosheets could be effectively decorated on the 1D semiconducting materials with rough surfaces and improved their interactions with the gas molecules, resulting in the improved gas-sensing performances of metal oxides.

The nanocomposite film composed of MoS_2 nanosheets-decorated Co_3O_4 nanorods was reported by Zhang et al. to be the potential to detect NH_3 with high performance [62]. Both the MoS_2 nanosheets and the Co_3O_4 nanorods were synthesized through a hydrothermal method with the temperature of 200 and 180 °C, respectively. Then the sensor based on the nanocomposite film was prepared via typical layer-by-layer (LBL) self-assembly. The prepared Co_3O_4 showed typical rod-like morphology with the measured average diameter being 98.15 nm. And the average size of the MoS_2 nanosheets was found to be 197.43 nm with good distribution. The sensor response ($\Delta R/R_{air}$*100%, $\Delta R = R_{air} - R_{gas}$) of nanocomposite film showed a close relationship with the number of self-assembled MoS_2/Co_3O_4 layers. The study showed that the sensor based on the five MoS_2/Co_3O_4 layers exhibited a more promising NH_3-sensing performance compared with the one with 1, 3, or 7 layers. The value of the sensor response of the five MoS_2/Co_3O_4 layers was 8.74% toward 0.1 ppm NH_3. Meanwhile, the nanocomposite film also showed good response performance to 1–6 ppm NH_3 with an excellent recovery property in the air atmosphere. The formation of the p–n heterojunction, the build of the potential barrier, and the bending of the energy bands would take place with the MoS_2 contacting with the Co_3O_4. The release of the free electrons and the recombination of holes in the Co_3O_4 in the nanocomposite modified the concentration of carries and the height of the potential barrier, which would be responsible for the superior NH_3-sensing property of the self-assembled MoS_2/Co_3O_4. The strategy and the method used in their work might also be applied to assemble metal oxides with other 2D nanomaterials with different layers to construct promising sensing material.

A sensor based on the MoS_2 nanosheets-decorated ZnO nanowires array was reported to effectively detect NO_2 at 200 °C [63]. A simple hydrothermal method was applied to prepare the ZnO nanowires array with a smooth surface. Then a layer of Mo was deposited on the surface of ZnO via a direct current (DC) magnetic sputtering. The Mo seed layers with different thicknesses were prepared via the magnetic sputtering with controlling the sputtering time, which was the source material that would be further used to synthesize MoS_2. The MoS_2 was grown with a chemical vapor deposition process at 770 °C. The authors investigated the effects of the working temperature on the NO_2-sensing performance. The sensor response

($\Delta R/R_{N2}$*100%, $\Delta R = R_{gas} - R_{N2}$) of the composite at 200 °C was found to be ~30%, approximately five times higher than that at room temperature (~6%). Meanwhile, the sensor response of the composite was highly dependent on the thickness of the MoS_2 nanosheets. The research showed that the composite with the magnetic sputtering time being five minutes exhibited a more outstanding NO_2-sensing performance compared with the other samples, showing a promising sensor response that was three times higher than that of the one with the sputtering time being one minute. As it was pointed out in the study, the thin MoS_2 layer persisted the conductive layer in the sensing material under the effect of interface depletion, which would result in poor sensitivity to NO_2. The too thick MoS_2 layer that made the depletion layers formed in the composite little effect the resistance of the MoS_2/ZnO nanowires. The enhanced sensing performance of the composite was attributed to the recombination of the electrons and the holes in the sensing material and the modification of the width of the depletion layer between the MoS_2 nanosheet and the ZnO nanowires. The uniform ZnO nanowires arrays were also a positive factor for the outstanding NO_2-sensing performance due to their role of channel for the transfer of carries, which could be a possible structure applied to improve the gas-sensing properties of metal oxides decorated with 2D nanosheets. The resistance of the sensor based on the prepared composited in their work was found to be unable to recover to the original level during the sensing process, which might indicate that the stability of the assembly sensor should be further explored and improved.

The 1D TiO_2 nanotubes decorated by 2D MoS_2 nanosheets, reported by Liang et al., were found to be sensing material to detect alcohol [64]. The TiO_2 nanotubes arrays were synthesized through anodization of untreated titanium foils with the water/ethylene glycol and NH_4F. The applied anodization voltage was 60 V with a time of two hours. The synthesized TiO_2 nanotubes were clearly in order with the average diameter and the average wall thickness of 120 and 20 nm, respectively. Then the small-size MoS_2 nanosheets were modified on the surface of the uniform TiO_2 nanotubes with the source materials being $MoCl_5$ and $Na_2S{\cdot}9H_2O$ through a hydrothermal method at 180 °C. The synthesized MoS_2 nanosheets increased the wall thickness of the nanotubes to be 90 nm. And the specific surface area of the TiO_2 nanotubes was also increased from the original value of 26.8–47.4 m^2/g when they were decorated with MoS_2 nanosheets, indicating the positive effects of MoS_2 on the TiO_2 nanotubes. The pure TiO_2 nanotubes exhibited n-type sensing performance to alcohol, while the ones decorated with MoS_2 nanosheets showed a contrary p-type sensing property. The n-type sensor response (R_{air}/R_{gas}) of the TiO_2 nanotubes was found to be only 1.3–100 ppm alcohol at 150 °C, so low that the TiO_2 nanotubes could not be effective to sense alcohol. When the TiO_2 nanotubes were decorated with MoS_2 nanosheets, the p-type sensor response (R_{gas}/R_{air}) was successfully improved to be as high as 14.2, further indicating the positive effects of MoS_2 on the sensing performance of TiO_2 nanotubes. It was reported the high surface area of the MoS_2 nanosheets, the fast transportation of electrons through vertical tube walls of TiO_2, and the formation of heterojunctions between them were the main factors to enhance the alcohol sensing of the composite. This research revealed that

the nanotubes array were effective channels for the carriers, and their gas-sensing performance could be positively improved via decorating with 2D nanomaterials.

The study of Li et al. also revealed that the MoS_2 nanosheets could be applied to effectively enhance the sensing response of Si nanowires to NO_2 at room temperature [65]. The silicon wafer was firstly cut and cleaned and then treated with 5% HF to remove the layer of silicon oxide layer on its surface. A layer of Ag nanoparticles was prepared on the surface of the treated silicon wafer. The Si nanowires array was obtained with a further chemical etching in the solution of HF and H_2O_2 at 30 °C. The results showed that the average length of the prepared Si nanowire was approximately 6 μm with a rough surface and clustered tip. To obtain the MoS_2-decorated Si nanowire, a layer of Mo was deposited on the surface of the Si nanowires via a DC magnetic sputtering and then was sulfurized through a method of the chemical vapor deposition with the temperature of 770 °C. The deposition rate of the MoS_2 nanosheets on the surface of Si nanowires was measured to be approximately 20 nm/min. It was reported that the gas-sensing performance of MoS_2-decorated Si nanowire with the deposition time being three minutes was superior compared with that of the one being deposited with the time of one or five minutes. The obtained MoS_2-decorated Si nanowires with the optimal deposition time exhibited promising sensing performance to NO_2 with different concentrations of 1–50 ppm It should be noted that the recovery process was found to be not fully completed during the sensing circle. The sensor response ($\Delta R/R_{N2}$*100%, $\Delta R = R_{gas} - R_{N2}$) of the Si nanowires was extremely improved through decorating with MoS_2 nanosheets. The sensor response of the composite was 28.4% toward 50 ppm NO_2, ~2.5 times higher than that of the pure Si nanowires (~10%). The MoS_2 nanosheets decorated on the Si nanowires introduced more active sites for the gas molecules, and the abundant S vacancies also facilitated the adsorptions of more NO_2 molecules on the composite. Furthermore, there would be a band bending taking place when the Si nanowires were composited with MoS_2, resulting in the formation of a potential barrier between their surfaces. The adsorption of NO_2 during the sensing process would capture the charges from the MoS_2 and then modify the height of the potential barrier in the composite, improving the sensing response of the composite. The authors have systematically studied the NO_2-sensing performance of the MoS_2-decorated Si nanowires and indicated that the MoS_2 could also be used to enhance the gas-sensing property of the semiconductor (not metal oxides).

11.2.3 WS_2-based Composite

The structure of the WS_2 was similar to that of the MoS_2 discussed ahead, which has been used to enhance the gas-sensing property of metal oxide. The sheet-like WS_2 was also applied to decorate metal oxide to effectively modify their gas-sensing property [66]. The gas-sensing performance of the ZnO nanorods was successfully enhanced via decorating them with uniform WS_2 nanosheets, which was reported by Fauzia and his group. In their work, a seed layer was prepared through a method of ultrasonic spray pyrolysis with the source material being Zn acetate dihydrate on the glass substrate. Then, a facile hydrothermal method was applied to grow the

uniform ZnO nanorods array with the raw materials being Zn nitrate tetrahydrate and hexamethylenetetramine at a low temperature of 95 °C for six hours. The WS_2 nanosheets were prepared via a probe sonication technique to exfoliate the nanosheets from the bulk WS_2. The obtained WS_2 was then spin-coated on the ZnO nanorods to assemble the composite (Figure 11.4a–f). Then the prepared composite was dried in air to obtain the stable gas sensor, as shown in Figure 11.4g. Meanwhile, the content of the WS_2 nanosheets was adjusted by modifying the deposition circles. There were two different composites assembled with the deposition circle being 1 or 3, named as ZnO/WS_2 1× or ZnO/WS_2 3×, respectively. The sensor response was defined as $(C_x - C_{18})/C_x$*100%, in which the C_x and the C_{18} represented the capacitance of the sensor in target humidity or 18% RH, respectively. The sensor response of the sensor based on pure ZnO or WS_2 to the humidity of 85% RH was 73.10 or 30.51, respectively. This sensor response was effectively improved to be 87.28 or 378.05 for ZnO/WS_2 1× or ZnO/WS_2 3×, respectively. The recovery time of the composite was almost the same as that of the pure ZnO or MoS_2, being in the range of 25.67–27.69 seconds (Figure 11.4h,i). While, the response times for ZnO/WS_2 1× or ZnO/WS_2 3× were calculated to be 41.38 or 74.51 seconds (Figure 11.4j,k), respectively. The humidity-sensing performance of the WS_2-decorated ZnO nanorods was reported to be attributed to the adsorption of water molecules on their surface. In the prepared composite, the WS_2 nanosheets also provided adsorption sites for the water molecules and made more gas molecules interact with the composite during the sensing process. And the authors also reported that the n–n heterojunction between the ZnO and WS_2 induced the establishment of an accumulation layer on one side of the ZnO/WS_2 interfaces, which would effectively increase the water dissociation rate. These two factors were mainly responsible for the improvement of the humidity-sensing property of the WS_2-decorated ZnO nanorods. This research indicated that the 2D WS_2 could also be the potential to enhance the gas-sensing performance of metal oxides.

Furthermore, the WS_2 nanosheets were found to be effective to enhance the NO_2-sensing performance of highly porous SiO_2 nanorods at room temperature (25 °C) [67]. The 1D SiO_2 nanorods were synthesized via a method of glancing angle deposition with an e-beam evaporator. The authors have deposited a series of SiO_2 nanorods with the same thickness of approximately 500 nm but different glancing angles of 75°, 77.5°, 80°, 82.5°, or 85°. The prepared SiO_2 nanorods were then treated with UV-O_3 cleaner and were further spin-coated with a solution of WCl_6. The WS_2 was decorated on the surface of the SiO_2 nanorods through a CVD system with two separated furnaces for sulfur and pretreated nanorods. The result showed that the WS_2 deposited at 85° presented a highly porous morphology. And the glancing angles also had significant effects on the NO_2-sensing performance of the SiO_2 nanorods at room temperature. The WS_2 deposited at 82.5° exhibited an optimal sensor response ($\Delta R/R_{gas}$*100%, $\Delta R = R_{air} - R_{gas}$) of 151.24% to 5 ppm NO_2 at room temperature, which was over six times higher than the bare WS_2 thin film (22.96%). Moreover, the sensor based on the WS_2 deposited at 82.5° also exhibited a promising sensing property to 400 ppb NO_2 with the theatrical detection limit being as low as 13.726 ppb. The enhanced NO_2 gas-sensing performance of the composite could be

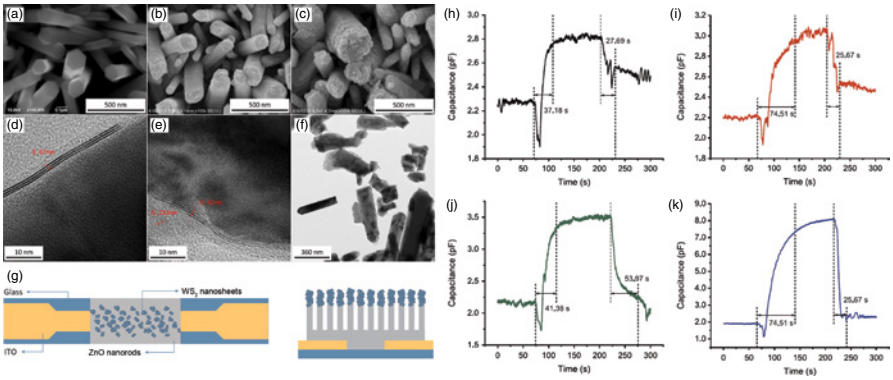

Figure 11.4 FESEM and TEM images of (a) ZnO, (b, d) ZnO/WS_2 1×, (c, e) ZnO/WS_2 3×, (g) the sketch of the assembled sensor, humidity sensing performance of sensor based on (h) WS_2, (i) ZnO, (j) ZnO/WS_2 1×, or (k) ZnO/WS_2 3×. Source: Dwiputra et al. [66], Reproduced with permission from Elsevier.

attributed to the highly porous structure of the vertically aligned SiO_2 nanorods decorated with WS_2 and the exposed edge sites of the WS_2. The porous structure and the high specific surface area of the composite facilitated more gas molecules diffused into the sensing material and adsorbed on its surface. And more edge sites of the WS_2 also enhanced the interaction between the gas molecule and the sensing substrate, further improving the NO_2-sensing performance of the SiO_2 nanorods decorated with WS_2. But only a few reports were focusing on this promising nanosheet up to now. More potential sensing materials could be constructed via decorating metal oxides with WS_2 nanosheets.

11.2.4 ZnO-based Composite

The ZnO nanosheet was also one of the popular 2D materials and has also been proved to be effective to improve the gas-sensing performance of 1D material. The investigation of Wang et al. revealed that the hydrogen-sensing performance of the Zn_2SnO_4 nanowires was effectively enhanced by decorating them with ZnO nanosheets [68]. In their work, the ZnO nanosheets decorated with Zn_2SnO_4 were prepared with a method of the metallic catalyst-assisted thermal evaporation of ZnO, SnO_2, and active carbon. A layer of Au with a thickness of 5 nm was firstly deposited on the surface of the substrate of the Si wafer via a sputtering method. Then a mixture of active carbon, ZnO, and SnO_2 powders was thermally evaporated to prepare the Zn_2SnO_4 decorated with ZnO at 800 °C with the pressure of 300 Torr in N_2, as shown in Figure 11.5a–c. Then a thin layer of Pd was also sputtered on the synthesized decorated Zn_2SnO_4 nanowires to assemble the gas sensor (Figure 11.5d–f). The result showed that the sensor based on the composite exhibited promising sensing performance toward 2–1000 ppm H_2 at the working temperature being 120, 200, 255, 270, or 300 °C (Figure 11.5g–j). The sensor response ($\Delta R/R_{air}$*100%, $\Delta R = R_{air} - R_{gas}$) of the sensor based on the ZnO-decorated Zn_2SnO_4 was 46% at the working temperature of 270 °C. With the sputtering of the Pd layer, the sensor response was further improved to be 74% and the working temperature was decreased to be 255 °C. The response time of the Pd-coated composite was 28 seconds to 1000 ppm H_2, also shorter compared to that of the bare ZnO-decorated Zn_2SnO_4 (41 seconds). And the Pd-coated composite exhibited excellent repeatability, selectivity, and long-term stability toward H_2, further indicating the potential of the composite in the area of hydrogen sensor. It should be noted that the sensor response of the composite was not high, which might be further improved to better meet the demands of practical application.

Meanwhile, Tian et al. have also synthesized a similar composite of ZnO-decorated Zn_2SnO_4 nanowire through a different method of a hydrothermal process combined with calcination [69]. The ZnO-decorated Zn_2SnO_4 nanowire in their research was reported to show outstanding sensing response to TEA at 200 °C. The raw materials of ZnO powder, $SnCl_4{\cdot}5H_2O$, and ZnOH were used to prepare the precipitates via a hydrothermal method at 200 °C for 20 hours. Then ZnO-decorated Zn_2SnO_4 nanowires were synthesized through annealing the obtained precipitates at 450 °C for two hours. The result showed there were numerous nanosheets contacted on the surface of the nanowires with an average diameter of 36.6 nm. And the

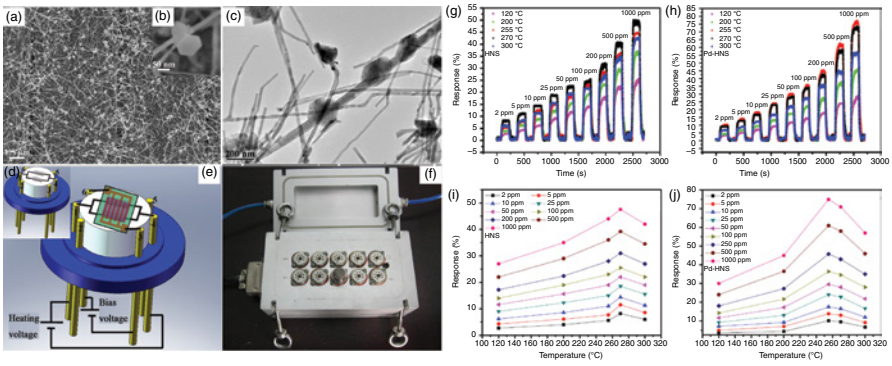

Figure 11.5 SEM images (a and b) and TEM image (c) of the ZnO-decorated Zn_2SnO_4 nanowires. The 3D schematic diagram of the heater (d) and the sensor (e), test gas chamber (f). The dynamic sensing performances of the sensor based on the ZnO-decorated Zn_2SnO_4 nanowires (g) and the Pd-decorated composite to 2–1000 ppm H_2 at various working temperatures (h). The relationship between the operating working temperature and the sensor response of the ZnO-decorated Zn_2SnO_4 nanowires (i) and the Pd-decorated composite (j). Source: Wang et al. [68], Reproduced with permission from Elsevier.

XRD pattern confirmed that the nanosheet and the nanowire in the composite were ZnO and Zn_2SnO_4 with the phase being hexagonal wurtzite and cubic spinel, respectively. The sensing response of the sensor based on the ZnO-decorated Zn_2SnO_4 was found to be effectively improved. The sensor response (R_{air}/R_{gas}) of the pure ZnO or Zn_2SnO_4 was 5.7 or 3.7, respectively, to 100 ppm TEA at 200 °C. Then the sensor response was improved to be 175.5 for the ZnO-decorated Zn_2SnO_4 nanowires. Moreover, the composite also exhibited promising sensing properties to 10–200 ppm TEA at 200 °C. The sensor response of the composite was 292.4–200 ppm TEA at 200 °C, so high indicating its great potential in the TEA sensor. And the sensor based on the composite also exhibited a short response time or recovery time to 100 ppm TEA, being 13 or 189 seconds, respectively. The special surface area of the composite was 19.11 m^2/g, over 1.5 times higher than that of the pure ZnO (12.49 m^2/g). The high special surface area would make more gas molecules adsorbed on the surface of the composite. The unique hierarchical structure of the composite also resulted in the establishment of a space charge layer and electron depletion layer, another factor being responsible for the improvement of the TEA sensing response. In addition, the building of heterojunction between the ZnO and the Zn_2SnO_4 would form an accumulation layer in the side of ZnO, making more oxygen molecules adsorbed and more charges captured. Therefore, the sensor based on the composite exhibited enhanced TEA sensing property.

Cho et al. have also constructed a novel sensor based on the heterojunctions of p-CuO nanowire and n-ZnO nanosheets [70]. The sensor based on the heterojunctions1 was found to show promising near-UV-sensing performance. According to the study of ZnO-decorated Zn_2SnO_4, the sensor based on the heterojunctions of p-CuO nanowire and n-ZnO nanosheets might also be the potential to exhibit outstanding gas-sensing performance under the UV.

Up to now, only a few researches were focusing on the improved gas-sensing performances of 1D nanostructures decorated with ZnO nanosheets. More attention should also be paid to this sheet-like metal oxide, because the ZnO has been proved to be effective to detect various gases. There would be more effective gas-sensing material assembled by decorating the metal oxides with 2D ZnO nanosheets.

11.2.5 NiO-based Composites

The NiO sheets with porous structures were reported to be positive to improve the gas-sensing performance of the ZnO nanorods [71]. The ZnO nanorods were synthesized with a hydrothermal method with source material of $Zn(CH_3COO)_2{\cdot}2H_2O$ and the PH of 10 at 180 °C for 14 hours. The NiO nanosheets were decorated on the surface of the prepared ZnO nanorods via a hydrothermal route with the source material being $NiCl_2{\cdot}6H_2O$ at a low temperature of 140 °C for 10 hours. The ZnO nanorods with a length of 1–3 μm were uniformly decorated with porous NiO nanosheets. The sensor was assembled via coating the paste composed of the prepared powders and deionized water on a ceramic tube. The sensor response of the pure ZnO (or NiO) was obtained to be 34.67 (or 85.88) to 100 ppm acetone at 200 °C (or 320 °C). Then the sensing performance of the NiO/ZnO composite was

significantly improved compared with the pure NiO or ZnO. The sensor based on the composite exhibited a high sensor response (R_{air}/R_{gas}) of 205.14–100 ppm acetone at the working temperature of 240 °C, which was two or six times higher than that of the pure ZnO or NiO, respectively. Moreover, the NiO/ZnO composite also showed a short response time or recovery time of 7 or 20 seconds, respectively, to 100 ppm acetone. In addition, the composite presented outstanding sensing selectivity toward acetone with sensing stability over 60 days. The larger specific surface area of the composite with more active sites facilitated the adsorptions of gas molecules on the sensing material compared with the pure ZnO or NiO. And the porous structure of the composite was also a positive factor improving the diffusion of gas molecules into the sensing materials. The formation of p–n heterojunction and the modulation of the width of the depletion layer between the interfaces between the NiO and ZnO made the resistance be changed more effectively, further resulting in the enhancement of the sensing response of the composite. The authors prepared a potential sensing material of NiO-decorated ZnO nanorods with promising acetone-sensing performance via a simple hydrothermal method. The working temperature was over 200 °C, which might be negative to full its application. There would have to be a heater in the sensor, increasing the power dissipation and the volume of the sensor. More attention should be paid to decreasing the working temperature of the composite, an issue to be overcome to further improve the comprehensive performances of sensors based on metal oxides.

The vertically aligned ZnO nanorods arrays decorated with 2D NiO nanosheets were, reported by Hur et al., effective to sense NO_2 [72]. The ZnO nanorods were synthesized with a hydrothermal method with the raw materials of diethanolamine, zinc acetate dehydrate, 2-methoxyethanol, zinc nitrate hexahydrate, and hexamethylenetetramine. A seed layer was firstly prepared on SiO_2/Si wafer, and then a hydrothermal process was conducted at a low temperature of 90 °C for five hours to synthesize the uniform ZnO nanorods array with the average diameter of ~800 nm. Then a layer of Ni seed was also preprepared on the surface of the ZnO nanorods and was further exposed to a mixed aqueous solution of nickel acetate tetrahydrate. Finally, the prepared composite was annealed in air at 400 °C to obtain the stable NiO-decorated ZnO. The growth time of the NiO showed a significant effect on the morphology of the composite, and there was also a close relationship between the content of NiO and the decorated ZnO nanorods. The sensor based on the decorated ZnO nanorods with the growth time of the NiO being 30 min exhibited the highest sensor response toward NO_2 among all the studied composites. The sensor response ($\Delta R/R_{gas}$*100%, $\Delta R = R_{gas} - R_{air}$) of the composites was calculated to be ~350%, which was three times or ~six times higher than that of the pure ZnO nanorods or NiO nanosheets, respectively. Meanwhile, the response time of the composite was also shorter compared with that of the NiO nanosheets. The surface area of the ZnO nanorods was effectively improved with the decoration of 2D NiO nanosheets, which was a positive factor that made more NO_2 molecules adsorbed on the surface of the composite. And there would be heterojunctions formed between ZnO and NiO, the electron depletion regions around which also adsorbing more NO_2 in the composite. In addition, the authors pointed out that the transfer of electrons and

holes between NiO and ZnO could maintain the adsorption of NO_2 on the surface of the composite, another factor being responsible for the enhanced NO_2-sensing performance of the ZnO nanorods decorated with NiO nanosheets. The method of preparing seed layers to synthesize the ZnO nanorods or the NiO nanosheets was an interesting and possible way to obtain uniform nanomaterials at low temperatures. The synthesizing temperature of the ZnO nanorods or the NiO nanosheets was 90 °C, paving a possible method to prepare the metal oxide and the 2D nanosheets at low temperatures.

Park et al. have fabricated a novel sensing material of WO_3 nanorods decorated with 2D NiO nanosheets and studied their potential sensing response toward acetaldehyde [73]. Their work revealed that the decorated NiO nanosheets could also be applied to decorate the WO_3 nanorods to improve their acetaldehyde sensing performance at 250 °C. A simple hydrothermal chemical route was applied to synthesize the composite. In their study, the NiO nanosheets were prepared via a hydrothermal process at 200 °C for 10 hours with the raw materials of $Ni(NO_3)_2{\cdot}6H_2O$ and NaOH. Then the WO_3 was synthesized with the $Na_2WO_4{\cdot}2H_2O$ and could be obtained with the hydrothermal method at 180 °C for 24 hours. The thickness of the prepared NiO was approximately 6 nm, and the average length and width of the WO_3 were reported to be 3.5 μm and 56 nm, respectively (Figure 11.6a,b). The composite was prepared by just mixing the obtained NiO nanosheets and the WO_3 nanorods. The composite with proportions of NiO nanosheets and WO_3 nanorods being 15 : 85 (NW2) exhibited a higher response to acetaldehyde compare the pure WO_3 and other composites with different proportions (Figure 11.6c,d). The decorated WO_3 with optimal proportion showed a promising sensing response to 20–100 ppm acetaldehyde at 250 °C with outstanding repeatability to 100 ppm acetaldehyde (Figure 11.6e–f). The sensor response ($\Delta R/R_{air}$*100%, $\Delta R = R_{gas} - R_{air}$) of the composite was 2184% to 100 ppm acetaldehyde at 250 °C with the response/recovery time being 1177/632 seconds. There would be n–p heterojunctions forming between the n-type WO_3 and the p-type NiO. The transfer of holes and electrons across their surfaces would form the depletion regions around heterojunctions and facilitate the adsorptions of oxygen gas molecules in the air and the target acetaldehyde molecules and improve their reactions. Then the released electrons recombined with the holes in the NiO, decreasing the net concentration of holes. The depletion region would also be widened with the migration of conduction electrons from WO_3. Then the sensing property of the sensor based on the NiO was effectively improved by decorating with WO_3. The WO_3 nanorods decorated with NiO nanosheets could be potential to effectively detect acetaldehyde with a relatively high sensor response. It would be better for the composite to decrease the sensor response time and recovery time, which should be overcome and be of great importance to further improve the application of sensors based on the metal oxides decorated with 2D NiO nanosheets.

11.2.6 Other 2D material-decorated 1D nanomaterial

The research of Zhang et al. revealed the ZnO nanoflowers, consisting of rod-like ZnO, decorated with Sb-doped SnO_2 nanosheets were effectively to detect NO_2 with

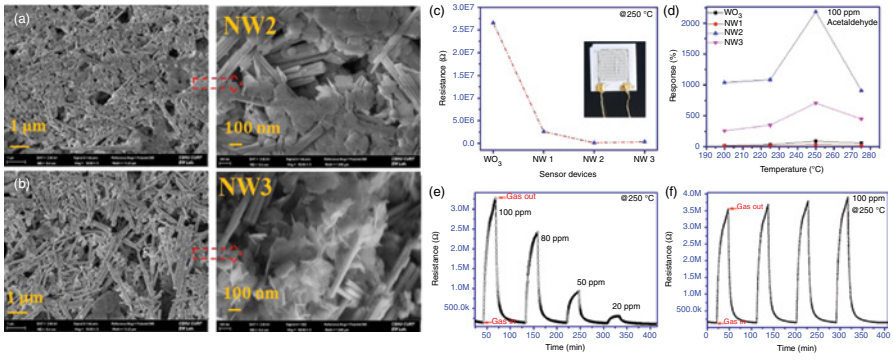

Figure 11.6 SEM images of NiO-decorated WO_3 with their proportions (wt%) being 15 : 85 (NW2, a) or 25 : 75 (NW3, b). (c) The resistance of the pure WO_3 or the composite with different proportions, the inset is the digital image of the assembled sensor. (d) The sensor response of the pure WO_3 or the composite under different working temperatures. (e) The dynamic sensing performance of NW2 sensor to 20–100 ppm acetaldehyde at 250 °C. (f) The sensing repeatability of NW2 to 100 ppm acetaldehyde at 250 °C. Source: Nakate et al. [73], Reproduced with permission from Elsevier.

low concentrations of 100–1000 ppb [74]. In the study, the ZnO nanorods were prepared with a microwaved hydrothermal method via raw materials being NaOH and $Zn(CH_3COO)_2{\cdot}2H_2O$ at 200 °C for 15 minutes. The obtained ZnO nanorods showed average length and diameter being ~6 μm and 500 nm, respectively. The Sb-doped SnO_2 nanosheets were then synthesized via a microwaved hydrothermal method. The morphology of the Sn-doped SnO_2 was significantly affected by the concentration of the doped Sn. The undoped SnO_2 exhibited typical nanowire-like morphology, but the morphology of the doped SnO_2 gradually changed to be nanosheets. It was observed that there were uniform SnO_2 nanosheets decorated on the surface of ZnO nanorods when the concentration of doped Sn was elevated to be 3%. The sensor response ($\Delta R/R_{N2}$, $\Delta R = R_{gas} - R_{N2}$) of the composites consisting of the Sb-doped SnO_2/ZnO heterojunctions increased with the increase of the doped Sb. The sensor response of the SnO_2/ZnO heterojunctions with the concentration of doped Sb being 7% was ~9.5 to 1000 ppb NO_2, one time higher than that of the one with the Sb being 1% (5.7). The response time of the composites of Sb being 7% was calculated to be only 16 seconds toward 1000 ppb NO_2, also shorter than that of the one with Sb of 1% (100 seconds). The sheet-like Sb-doped SnO_2 provided more active sites for the gas adsorption compared with the nanowire-like SnO_2. And more NO_2 was also adsorbed on the surface of the doped SnO_2 when the Sn^{4+} was replaced by Sb^{5+} or Sb^{3+}. Therefore, there would be more gas molecules adsorbed on the surface of the ZnO nanorods decorated with Sb-doped SnO_2 nanosheets during the response and recovery process, resulting in the enhanced gas-sensing performance of the heterojunctions. This study provided a possible and fast way to synthesize the 1D metal oxides decorated with 2D metal oxides, which would be promising to design novel sensing materials with heterostructure to exhibit outstanding sensing material.

Vertically ultrathin SnO_2 nanosheets were also grown *in situ* on the quasi-1D SiC nanofibers to form hierarchical architecture by a two-step method [75]. The SiC nanofibers were firstly prepared and then was immersed into the precursor with the raw material of $SnCl_2{\cdot}2H_2O$ to synthesize the SnO_2 nanosheet-decorated SiC via a simple hydrothermal process at 100–180 °C for six hours. Finally, the samples were calcined at 600 °C for two hours to obtain the SnO_2 nanosheet-decorated SiC nanofibers. The sensor based on the composited showed a sensor response (R_{air}/R_{gas}) of ~23 toward 100 ppm ethanol at 350 °C with the response time and the recovery time being four and six seconds, respectively. Furthermore, the hierarchical composite also exhibited a superior gas-sensing performance including high sensor response, excellent repeatability, and outstanding selectivity toward ethanol among the target gases. This work highlighted the possibility to develop a novel high-performance gas sensor based on 1D/2D hybrids used in harsh environments.

Wang et al. have reported a sensor based on Pt single atoms-decorated SnO_2 nanorods-loaded on SiC nanosheets with excellent C_2H_5OH-sensing property at 350 °C [76]. The SiC nanosheets were synthesized with a method of carbothermal reduction with the raw materials of Si powder and GO. Then the prepared SiC nanosheets were further treated by a hydrothermal reaction at 150 °C for the loading of abundant active sites (–OH). The functional SiC nanosheets could be a possible substrate for anchoring SnO_2 nanorods on their surfaces via a one-step colloidal

synthesis. The formed SnO_2 nanorods showed an average length and diameter of 8 and 2 nm, respectively (Figure 11.7a,b). Finally, the Pt single atoms were decorated on the SnO_2-loaded SiC nanosheets through a wet impregnation method combined with carefully controlling the concentration of H_2PtCl_6 in the prepared precursor. An aberration-corrected high-angle annular dark-field scanning transmission electron microscopy (HAADF-STEM) clearly illustrated that the dispersed Pt was 0.1–0.2 nm (Figure 11.7c), reasonably indicating that the single-atom Pt was successfully synthesized in the composite. The exquisite structure and the highly active Pt composite (Figure 11.7d) showed excellent gas-sensing performance at 350 °C with a high sensor response (R_{air}/R_{gas}) of 119.75 ± 3.90 toward 500 ppm ethanol (Figure 11.7e). Meanwhile, the Pt-decorated SnO_2-loaded SiC nanosheets also exhibited a promising sensor response of ~1.4 to 500 ppb ethanol with the response time and recovery time of ~14 and ~20 s (Figure 11.7f,g), respectively, further inferring the potential application of the composite to detect ethanol. Additionally, the sensor based on the prepared composite also exhibited outstanding sensing repeatability, long stability, and selectivity to ethanol at 350 °C (Figure 11.7h–j). The enhanced ethanol sensing property of the composite was mainly attributed to the formation of heterojunctions, the high-catalytic single-atom Pt for facilitating the generation of negative oxygen species, the large specific surface area, and the abundant active sites in the composite. This research revealed that the gas-sensing property of the SnO_2-based materials could be enhanced with the help of single-atom Pt. In addition, the facile method to efficiently synthesize the single-atom Pt and the design of novel ternary sensing material is also a possible way to assemble gas sensors with exciting sensing properties.

Xu and his workmates have synthesized the MoO_3 nanorods and then decorated them with porous $NiCO_2O_4$ nanosheets to improve their ethanol sensing performance [77]. The uniform MoO_3 nanorods were prepared via a hydrothermal method with the source material of Mo powder and H_2O_2 at 180 °C for 24 hours. The obtained MoO_3 exhibited typical rod-like morphology with a clean surface. The average length or width of the MoO_3 nanorods was reported to be approximately 20 μm or 200 nm, respectively. The uniform MoO_3 nanorods were then decorated with porous $NiCO_2O_4$ nanosheets through a route of chemical deposition with the $Ni(NO_3)_2{\cdot}6H_2O$, 2 mmol $Co(NO_3)_2{\cdot}6H_2O$, and 15 mmol $CO(NH_2)_2$ at 95 °C for two hours. The decoration of $NiCO_2O_4$ nanosheets increased the width of the MoO_3 nanorod to be 500 nm, and the composite was well dispersed with porous surfaces (Figure 11.8a–h). The sensor based on the composite exhibited a typical p-type sensing performance toward ethanol with the concentration of 50–1000 ppb at 350 °C (Figure 11.8i). However, the pure MoO_3 nanorods or the bare $NiCO_2O_4$ nanosheets exhibited no obvious sensing response to the ethanol vapor, indicating their poor sensing property. The sensor response (R_{gas}/R_{air}) of the composite to 50 ppb ethanol was 2.7, and the sensor response was increased to be 20 when the concentration of ethanol was increased to be 1000 ppb (Figure 11.8j). Moreover, the composite also showed excellent sensing repeatability and stability to ethanol with high selectivity. The special surface area of the MoO_3 nanorods was effectively increased when they were decorated with $NiCO_2O_4$ nanosheets, which would fascinate more oxygen molecules chemically adsorbed on their surfaces. And the porous structure of the composite

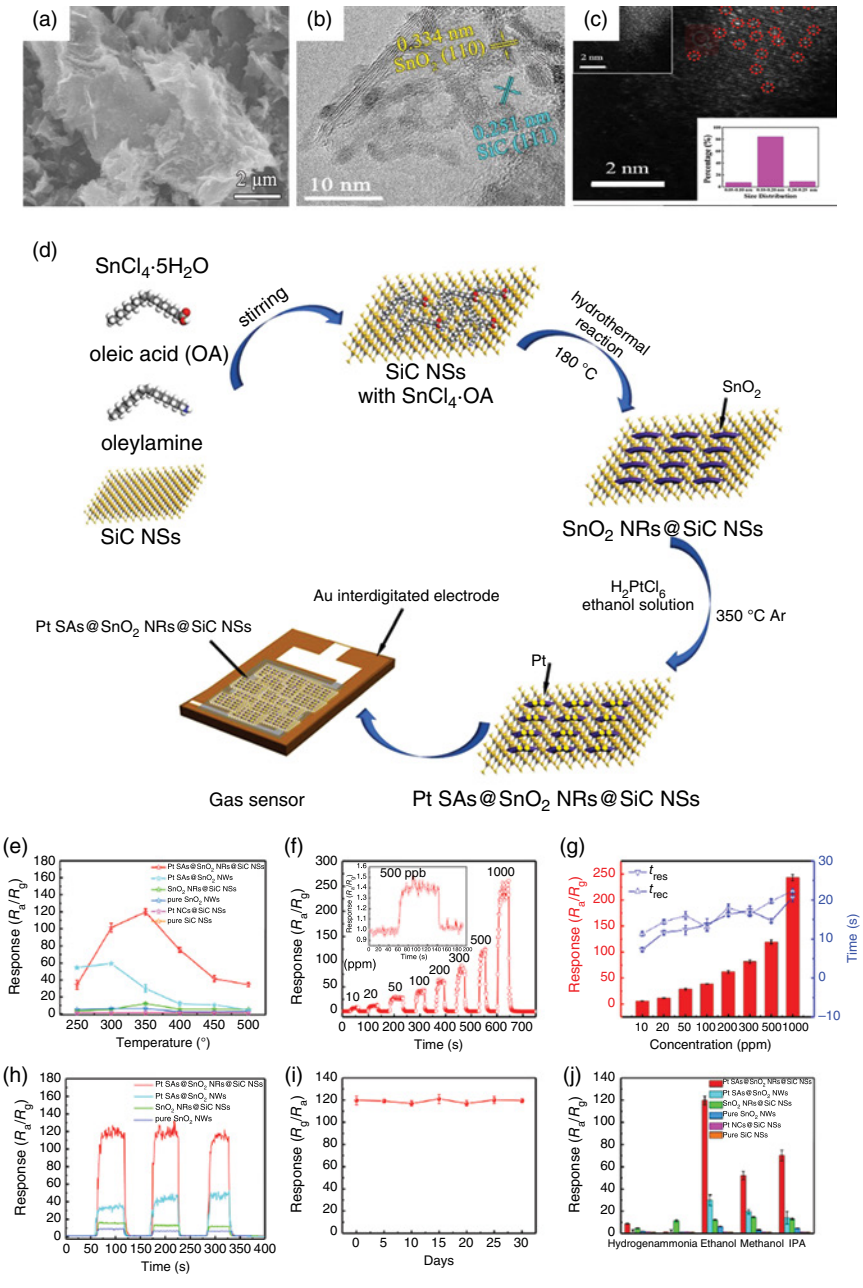

Figure 11.7 (a) SEM image, (b) TEM image, and (c) high-resolution HAADF-STEM images of Pt single atoms-decorated SnO_2 nanorods loaded on SiC nanosheets. (d) The sketch of the process to synthesize the composite and assemble the gas sensor. (e–j) The corresponding gas-sensing performances of the sensors based on the synthesized sensing materials at 350 °C. Source: Sun et al. [76], Reproduced with permission from American Chemical Society.

could be another positive factor for the gas adsorption and diffusion, which would further improve the gas-sensing performance. It was reported that the heterojunctions between $NiCO_2O_4$ and α-MoO_3 would promote the chemical adsorption of oxygen molecules on MoO_3 due to the existence of an electron accumulation layer with a high electron concentration. Then more electrons were captured in MoO_3, and this process would also make more electrons transferred from $NiCO_2O_4$, increasing the hole concentration of holes in the side of $NiCO_2O_4$ and resulting in the low resistance of the composite in air. When the ethanol was introduced, the reaction between the promoted chemisorbed oxygen species and the ethanol would release more electrons back to the composite than the pure MoO_3, significantly decreasing the hole concentration in $NiCO_2O_4$ and improving the sensor response of the composite. In the research, the effect of the content of the decorated $NiCO_2O_4$ was not reported, an important factor to fully understand the sensing performance of the composite. The sensor based on the composited with optimal content of $NiCO_2O_4$ might be exhibited a higher sensor response to ethanol at a lower working temperature (Figure 11.8).

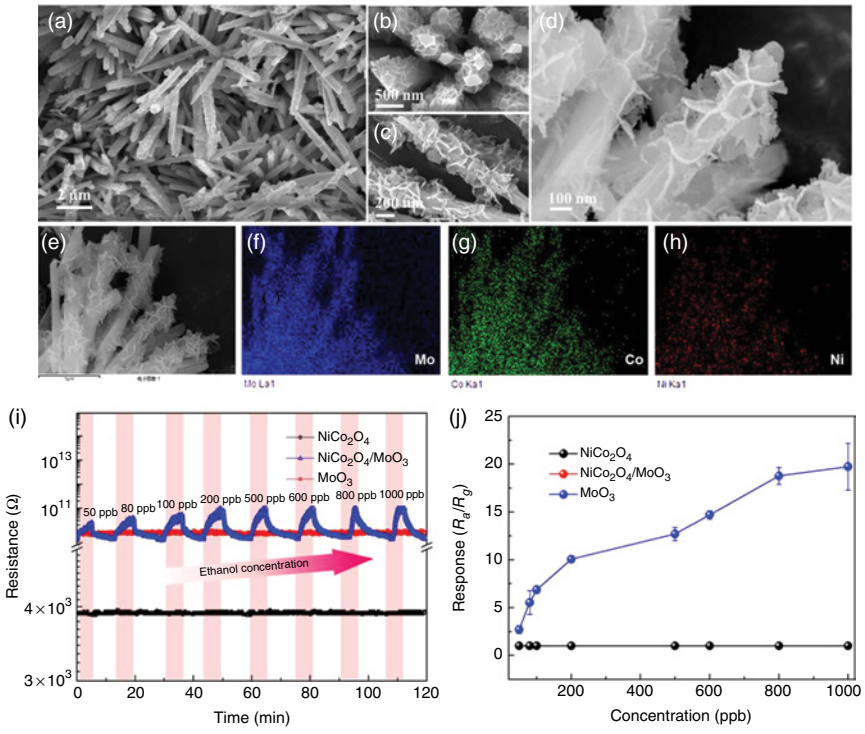

Figure 11.8 (a–d) SEM images, (e) TEM image, and (f–h) corresponding elemental mapping images of MoO_3 nanorods decorated with porous $NiCO_2O_4$ nanosheets. (i) Dynamic sensing performance of pure MoO_3 nanorods, bare $NiCO_2O_4$ nanosheets, or the $NiCO_2O_4$-decorated MoO_3 nanorods to 50–1000 ppb to ethanol at 350 °C. The assembled sensor is similar to that shown in the inset in Figure 11.6c. (j) The corresponding concentration-dependent gas sensor response of $NiCO_2O_4$-decorated MoO_3 nanorods. Source: Xu et al. [77], Reproduced with permission from Elsevier.

The study of Xu et al. showed that the novel heterostructure of Co_3O_4 nanowire array modified with $ZnSnO_3$ nanosheets was fabricated in situ on flat alumina substrates with Pt interdigitated electrodes and Pt heaters via a simple hydrothermal method without seed layers [78]. The gas-sensing measurement revealed that the Co_3O_4–$ZnSnO_3$ composite arrays showed a sensor response of 5.57 (R_{gas}/R_{air}) toward 100 ppm ethanol at 300 °C, which was 2.04 times higher than that of Co_3O_4 nanowire arrays. A similar structure of Co_3O_4 nanowires decorated with $NiMoO_4$ nanosheets was also established via a similar method by the same team [79]. The sensor based on the $NiMoO_4$-decorated Co_3O_4 nanowire array was also exhibited a higher sensor response of 17.12 toward 100 ppm trimethylamine at 250 °C, 3.91 times higher than that of Co_3O_4 arrays (4.39).

The work of Wang and his team revealed that the composite film of few-layer black phosphorus nanosheets and ZnO nanowires could be utilized to detect NO_2 at room temperature [80]. The black phosphorus nanosheets were synthesized via an exfoliation method, and the composite was prepared via mixing the black phosphorus nanosheets and the ZnO nanowires. The sensor response ($\Delta R/R_{air}$*100%, $\Delta R = R_{gas} - R_{air}$) of the pure black phosphorus nanosheets was reported to be only 37.7% to 50 ppb NO_2 at 25 °C. Then the sensing performance of the composite was effectively enhanced with a higher sensor response of 74% to the NO_2 with the same concentration.

The g-C_3N_4 nanosheets were also applied to modify the SnO_2 nanorods to successfully improve their ethanol sensing response [81]. The flower-like SnO_2/g-C_3N_4 nanocomposites were synthesized via a facile hydrothermal method with the source materials of $SnCl_4 \cdot 5H_2O$ and urea. It was found that the composite with the content of g-C_3N_4 being 7 wt% showed a better sensing performance toward ethanol compared with that of the one composited with the content of g-C_3N_4 being 0, 5, or 9 wt%. The composite with the optimal content exhibited a sensor response (R_{air}/R_{gas}) of 1150–500 ppm ethanol at 340 °C, three times higher than that of the pure SnO_2 (43). In addition, the working temperature was also decreased from the original 360 °C for the pure SnO_2 nanowires to 340 °C for the composite.

These researches illustrated that a majority of the reported 1D/2D hybrids could be effectively assembled via a two-step method. And the sensing response and the working temperature of the 1D sensing material were successfully improved through decorated 2D sheet-like materials. However, there are still some challenges remaining to be overcome to improve the gas-sensing performance of the 1D/2D composite, which would be discussed in detail in the following texts.

11.3 Remain Challenges and Possible Effective Ways to Explore High-Performance Gas Sensor

In general, the sensor responses of a majority of the sensors based on the 1D/2D hybrids always increase with increasing the working temperature. The highest value of the sensor response of the sensor could be obtained at an optimal working temperature. Then the sensor response would decrease with further increasing the

working temperature over the optimal value. However, the 1D/2D hybrids could only exhibit a high sensor response to target gas at a relatively high optimal working temperature. For example, the sensor response of the RGO-loaded CuO nanofibers was improved to 11.7–100 ppm H_2S of at the optimal working temperature of 300 °C [82]. The sensor based on the ZnO nanofibers loaded by RGO with the weight percent being 0.44 wt% presented the optimal NO_2-sensing performance at 400 °C [83]. As discussed in the section of **Introduction**, there would be a high risk of explosion when the concentration of the gas was increased to be in the explosive limit. The high working temperature would make the explosion more likely to take place and increase the power consumption of the gas sensor. The low working temperature might not provide enough energy that makes the oxygen species react with the target gas, but the high working temperature might accelerate the desorption of the oxygen species or the target gas, which was responsible for the highest sensor response at an optimal working temperature [47]. Further modification of the sensing material with certain catalysts might be possible to decrease the energy required to trigger the reaction between the oxygen species and the target gas. The Pt or Pd has been successfully used to decrease the working temperature of the sensor based on metal oxides. The optimal working temperature of the MoO_3 was decreased from 250 to 175 °C with the decoration of Pt and graphitic-carbon nitride (g-CN) [84]. Even though the decoration of noble metal nanoparticles might increase the cost of production, the low working temperature could decrease the power consumption and effectively reduce the explosion risk during the operating of the gas sensors based on the 1D/2D hybrids.

Another challenge for the reported sensors based on the 1D/2D hybrids is that they are still significantly affected by the humidity. It was reported that the adsorbed oxygen species or the target gas molecules on the surface of the sensing materials played an important role in the sensing response. The reaction between the oxygen species and the target gas was responsible for the sensing response of the sensor. The sensor response always decreased with increasing humidity, widely described as water vapor poisoning [79, 85]. When the sensor worked under high humidity, the adsorption of water molecules on the surface of the sensing material would decrease the active site for the adsorption of oxygen molecules in the air, then the number of the adsorbed oxygen species would decrease and fewer target molecules would consume during the sensing process, leading to the decrease in the sensor response. Meanwhile, the adsorbed water molecules might directly react with oxygen species (O^-) to form terminal hydroxyl groups on the surface of the sensing material, and the target gas molecule would also have to compete with the adsorbed water molecule and the target molecule, another factor responsible for the decreased sensor response under high humidity. Additionally, the sensor response of the 1D metal oxide-based sensor was found to be slightly weakened in 30–60 days, reported in several references [36, 86]. This might also be attributed to the decreased active sites on the surface of the sensing material with the fluctuation of humidity and the adsorptions of water molecules. The method of designing the corresponding compensating circuit, doping metal oxides with metal atom, coating the sensing material with hydrophobic polymer, or functionalizing the

sensing substrate with metal nanoparticles might be possible and successful to minimize or reduce the effect of humidity on the gas sensing performance of the 1D metal oxides composited with 2D materials [87–90]. The structure of the gas-sensing device would become complex to some extent, but the negative effects of the humidity on the gas-sensing properties of metal oxides-based sensors could be effectively limited or even eliminated. It should be noted that there were few reports systematically investigating the effective strategy to improve the stability of the metal oxide-based sensor under high humidity. More efforts should be made to study and explore the method to possibly avoid the effects of humidity on the gas-sensing performance of 1D/2D hybrids, meaningful to further promote the application of gas sensors.

Our discussions aforementioned revealed that the gas-sensing performance of 1D semiconducting material with the morphology of nanorod, nanowire, or nanofiber could be successfully enhanced through compositing with 2D nanosheets of graphene, GO, MoS_2, WS_2, ZnO, NiO, SnO, or $NiCO_2O_4$. It was clear that only a few kinds of 2D nanosheets were used to improve the 1D metal oxide. The sheet-like BN, In_2O_3, TiC, Co_3O_4, or InSe were also reported to be potential gas-sensing materials [91–95]. These 2D nanosheets might be applied to decorated 1D metal oxides to improve their gas-sensing responses. With more and more 1D/2D composite designed and constructed, it might be possible to assemble the gas sensor with high sensor response, short response/recovery time, and outstanding long-term stability at low working temperature and under high humidity. The relatively poor sensing performance of some reported 1D/2D composite might also indicate that the selected sensing material was not the optimal one. The latest 2D sheet-like materials could be a candidate to assemble potential sensing substrate to exhibit promising gas-sensing performance.

Recently, the method of machine learning and high-throughput computing has been widely and popularly used to efficiently explore possible high-performance materials in the area of drug discovery, diagnostic system for complex diseases, toxicity assessment, or gas sensors [96–99]. Meanwhile, machine learning was also applied to explore the selectivity of E-nose with plenty of data labeled under various circumstances [100–102]. The work of Salhi et al. suggested that machine learning was effective to develop high-performance smart e-nose with seven sensors to realize the early detection of gas leakage [103]. The trained smart e-nose was reported to be successful in selectively sensing LPG, CO, CO_2, smoke, or flame under different humidity conditions with the accuracy being almost 100%. Therefore, the potential sensing material could be effectively selected from the database with high-throughput screening certain conditions. The selected sensing substrate would test to label enough data under various environments to obtain a dataset. The assembled sensor might be likely to exhibit high sensor response and short response/recovery time with promising selectivity with further training of the collected dataset. According to the discussions aforementioned, the method of machine learning combined with high-throughput computing could be a successful method to effectively screen potential sensing materials and train the dataset to further improve their gas-sensing properties [104, 105]. More attention should be paid to this efficient strategy to develop high-performance gas sensors to better meet the

requirements of practical applications. The gas sensor based on 1D/2D hybrids is now in the ascendant, and one can envision a bright prospect for the development of this promising composite.

11.4 Conclusions

The 1D metal oxide with the structure of nanowire, nanorod, or nanofiber has been widely applied as sensing material to detect various gases. And their gas-sensing performance could be effectively enhanced through compositing them with 2D sheet-like materials. The typical 2D material of graphene-based nanosheets, MoS_2, WS_2, NiO, ZnO, SnO_2, SiC, $NiCO_2O_4$, or g-C_3N_4 have been successfully decorated on the 1D sensing material to improve their sensing responses. The high special surface area, the establishment of heterojunction, and the modulation of the potential barrier are mainly responsible for the enhanced gas-sensing performances of 1D semiconducting nanostructures decorated with 2D materials. The relatively high working temperature and the weakened gas-sensing property under high humidity might limit the further application of the 2D material-decorated 1D metal oxide in practices. The high-throughput computing with further machine learning could be a possible strategy to screen more effective gas-sensing material to exhibit more outstanding gas-sensing performance.

Acknowledgments

This work was financially supported by the National Natural Science Foundation of China (Grant no. 51802109 and 51972102) and the Department of Education of Hubei Province (Grant no. D20202903).

References

1 Ma, X., Jia, H., Sha, T. et al. (2019). Spatial and seasonal characteristics of particulate matter and gaseous pollution in China: implications for control policy. *Environ. Pollut.* 248: 421–428.
2 Wen, M., Li, G., Liu, H. et al. (2019). Metal–organic framework-based nanomaterials for adsorption and photocatalytic degradation of gaseous pollutants: recent progress and challenges. *Environ. Sci.: Nano* 6: 1006–1025.
3 Guan, W., Tang, N., He, K. et al. (2020). Gas-sensing performances of metal oxide nanostructures for detecting dissolved gases: a mini review. *Front. Chem.* 8: 76.
4 Cho, S.H., Suh, J.M., Eom, T.H. et al. (2021). Colorimetric sensors for toxic and hazardous gas detection: a review. *Electron. Mater. Lett.* 17: 1–17.
5 Buckley, D.J., Black, N.C., Castanon, E.G. et al. (2020). Frontiers of graphene and 2D material-based gas sensors for environmental monitoring. *2D Mater.* 7: 032002.

6 Umar, A., Ibrahim, A.A., Nakate, U.T. et al. (2021). Fabrication and characterization of CuO nanoplates based sensor device for ethanol gas sensing application. *Chem. Phys. Lett.* 763: 138204.

7 Vanotti, M., Poisson, S., Soumann, V. et al. (2021). Influence of interfering gases on a carbon monoxide differential sensor based on SAW devices functionalized with cobalt and copper corroles. *Sens. Actuators, B* 332: 129507.

8 Yang, S., Lei, G., Xu, H. et al. (2019). A DFT study of CO adsorption on the pristine, defective, In-doped and Sb-doped graphene and the effect of applied electric field. *Appl. Surf. Sci.* 480: 205–211.

9 Zou, M., Aono, Y., Inoue, S., and Matsumura, Y. (2020). Response of palladium and carbon nanotube composite films to hydrogen gas and behavior of conductive carriers. *Materials* 13: 4568.

10 Dong, M., Zheng, C., Miao, S. et al. (2017). Development and measurements of a mid-infrared multi-gas sensor system for CO, CO_2 and CH_4 detection. *Sensor* 17: 2221.

11 Tang, H., Sacco, L.N., Vollebregt, S. et al. (2020). Recent advances in 2D/nanostructured metal sulfide-based gas sensors: mechanisms, applications, and perspectives. *J. Mater. Chem.* 8: 24943–24976.

12 Zhao, C., Gong, H., Niu, G., and Wang, F. (2020). Ultrasensitive SO_2 sensor for sub-ppm detection using Cu-doped SnO_2 nanosheet arrays directly grown on chip. *Sens. Actuators, B* 324: 128745.

13 Li, K., Luo, Y., Liu, B. et al. (2019). High-performance NO_2-gas sensing of ultrasmall $ZnFe_2O_4$ nanoparticles based on surface charge transfer. *J. Mater. Chem.* 7: 5539–5551.

14 Lou, C., Yang, C., Zheng, W. et al. (2021). Atomic layer deposition of ZnO on SnO_2 nanospheres for enhanced formaldehyde detection. *Sens. Actuators, B* 329: 129218.

15 Arafat, M., Dinan, B., Akbar, S.A., and Haseeb, A. (2012). Gas sensors based on one dimensional nanostructured metal-oxides: a review. *Sensor* 12: 7207–7258.

16 Fu, X., Yang, P., Xiao, X. et al. (2019). Ultra-fast and highly selective room-temperature formaldehyde gas sensing of Pt-decorated MoO_3 nanobelts. *J. Alloys Compd.* 797: 666–675.

17 Kumar, R., Al-Dossary, O., Kumar, G., and Umar, A. (2015). Zinc oxide nanostructures for NO_2 gas–sensor applications: a review. *Nano-Micro Lett.* 7: 97–120.

18 Park, K.-R., Cho, H.-B., Lee, J. et al. (2020). Design of highly porous SnO_2-CuO nanotubes for enhancing H2S gas sensor performance. *Sens. Actuators, B* 302: 127179.

19 Seiyama, T., Kato, A., Fujiishi, K., and Nagatani, M. (1962). A new detector for gaseous components using semiconductive thin films. *Anal. Chem.* 34: 1502–1503.

20 Miller, D.R., Akbar, S.A., and Morris, P.A. (2014). Nanoscale metal oxide-based heterojunctions for gas sensing: a review. *Sens. Actuators, B* 204: 250–272.

21 Govardhan, K. and Grace, A.N. (2016). Metal/metal oxide doped semiconductor based metal oxide gas sensors-a review. *Sens. Lett.* 14: 741–750.

22 Wang, Z., Hu, Y., Wang, W. et al. (2012). Fast and highly-sensitive hydrogen sensing of Nb_2O_5 nanowires at room temperature. *Int. J. Hydrogen Energy* 37: 4526–4532.

23 Song, Y.G., Park, J.Y., Suh, J.M. et al. (2018). Heterojunction based on Rh-decorated WO_3 nanorods for morphological change and gas sensor application using the transition effect. *Chem. Mater.* 31: 207–215.

24 Tao, K., Han, X., Yin, Q. et al. (2017). Metal-organic frameworks-derived porous In_2O_3 hollow nanorod for high-performance ethanol gas sensor. *ChemistrySelect* 2: 10918–10925.

25 Wang, C., Cui, X., Liu, J. et al. (2016). Design of superior ethanol gas sensor based on Al-doped NiO nanorod-flowers. *ACS Sens.* 1: 131–136.

26 Wang, X., Wang, T., Si, G. et al. (2020). Oxygen vacancy defects engineering on Ce-doped α-Fe_2O_3 gas sensor for reducing gases. *Sens. Actuators, B* 302: 127165.

27 Tonezzer, M. (2019). Selective gas sensor based on one single SnO_2 nanowire. *Sens. Actuators, B* 288: 53–59.

28 Liu, W., Xu, L., Sheng, K. et al. (2018). A highly sensitive and moisture-resistant gas sensor for diabetes diagnosis with Pt@ In_2O_3 nanowires and a molecular sieve for protection. *NPG Asia Mater.* 10: 293–308.

29 Li, Z. (2017). Supersensitive and superselective formaldehyde gas sensor based on NiO nanowires. *Vacuum* 143: 50–53.

30 Naama, S., Hadjersi, T., Keffous, A., and Nezzal, G. (2015). CO_2 gas sensor based on silicon nanowires modified with metal nanoparticles. *Mater. Sci. Semicond. Process.* 38: 367–372.

31 Yang, S., Lei, G., Xu, H. et al. (2021). Metal oxide based heterojunctions for gas sensors: a review. *Nanomaterials* 11: 1026.

32 Ge, L., Mu, X., Tian, G. et al. (2019). Current applications of gas sensor based on 2-D nanomaterial: a mini review. *Front. Chem.* 7: 839.

33 Kumar, R., Liu, X., Zhang, J., and Kumar, M. (2020). Room-temperature gas sensors under photoactivation: from metal oxides to 2D materials. *Nano-Micro Lett.* 12: 1–37.

34 Choi, S.-J. and Kim, I.-D. (2018). Recent developments in 2D nanomaterials for chemiresistive-type gas sensors. *Electron. Mater. Lett.* 14: 221–260.

35 Wang, C.N., Li, Y.L., Gong, F.L. et al. (2020). Advances in doped ZnO nanostructures for gas sensor. *Chem. Rec.* 20: 1553–1567.

36 Moon, D.-B., Bag, A., Lee, H.-B. et al. (2021). A stretchable, room-temperature operable, chemiresistive gas sensor using nanohybrids of reduced graphene oxide and zinc oxide nanorods. *Sens. Actuators, B* 345: 130373.

37 Zhao, Y., Li, H., Li, Y. et al. (2021). Layered SnO_2 nanorods arrays anchored on reduced graphene oxide for ultra-high and ppb level formaldehyde sensing. *Sens. Actuators, B* 346: 130452.

38 Xu, K., Yang, L., Yang, Y., and Yuan, C. (2017). Improved ethanol gas sensing performances of a ZnO/Co_3O_4 composite induced by its flytrap-like structure. *Phys. Chem. Chem. Phys.* 19: 29601–29607.

39 Novoselov, K.S., Geim, A.K., Morozov, S.V. et al. (2004). Electric field effect in atomically thin carbon films. *Science* 306: 666–669.

40 Chatterjee, S.G., Chatterjee, S., Ray, A.K., and Chakraborty, A.K. (2015). Graphene–metal oxide nanohybrids for toxic gas sensor: a review. *Sens. Actuators, B* 221: 1170–1181.

41 Toda, K., Furue, R., and Hayami, S. (2015). Recent progress in applications of graphene oxide for gas sensing: a review. *Anal. Chim. Acta* 878: 43–53.

42 Majhi, S.M., Mirzaei, A., Kim, H.W., and Kim, S.S. (2021). Reduced graphene oxide (rGO)-loaded metal-oxide nanofiber gas sensors: an overview. *Sensor* 21: 1352.

43 Rafiee, Z., Roshan, H., and Sheikhi, M.H. (2021). Low concentration ethanol sensor based on graphene/ZnO nanowires. *Ceram. Int.* 47: 5311–5317.

44 Minh Triet, N., Thai Duy, L., Hwang, B.-U. et al. (2017). High-performance Schottky diode gas sensor based on the heterojunction of three-dimensional nanohybrids of reduced graphene oxide–vertical ZnO nanorods on an AlGaN/GaN layer. *ACS Appl. Mater. Interfaces* 9: 30722–30732.

45 Yang, S., Wang, Z., Zou, Y. et al. (2017). Remarkably accelerated room-temperature hydrogen sensing of MoO_3 nanoribbon/graphene composites by suppressing the nanojunction effects. *Sens. Actuators, B* 248: 160–168.

46 Abideen, Z.U., Kim, H.W., and Kim, S.S. (2015). An ultra-sensitive hydrogen gas sensor using reduced graphene oxide-loaded ZnO nanofibers. *Chem. Commun.* 51: 15418–15421.

47 Yan, C., Lu, H., Gao, J. et al. (2018). Improved NO_2 sensing properties at low temperature using reduced graphene oxide nanosheet-In_2O_3 heterojunction nanofibers. *J. Alloys Compd.* 741: 908–917.

48 Galstyan, V., Ponzoni, A., Kholmanov, I. et al. (2018). Reduced graphene oxide-TiO_2 nanotube composite: comprehensive study for gas-sensing applications. *ACS Appl. Nano Mater.* 1: 7098–7105.

49 Sun, Z., Huang, D., Yang, Z. et al. (2015). ZnO nanowire-reduced graphene oxide hybrid based portable NH_3 gas sensing electron device. *IEEE Electron Device Lett.* 36: 1376–1379.

50 Meng, H., Yang, W., Ding, K. et al. (2015). Cu_2O nanorods modified by reduced graphene oxide for NH_3 sensing at room temperature. *J. Mater. Chem. A* 3: 1174–1181.

51 Chu, X., Hu, T., Gao, F. et al. (2015). Gas sensing properties of graphene–WO_3 composites prepared by hydrothermal method. *Mater. Sci. Eng., B* 193: 97–104.

52 Bai, S., Chen, C., Luo, R. et al. (2015). Synthesis of MoO_3/reduced graphene oxide hybrids and mechanism of enhancing H_2S sensing performances. *Sens. Actuators, B* 216: 113–120.

53 Xia, Y., Wang, J., Xu, J.-L. et al. (2016). Confined formation of ultrathin ZnO nanorods/reduced graphene oxide mesoporous nanocomposites for high-performance room-temperature NO_2 sensors. *ACS Appl. Mater. Interfaces* 8: 35454–35463.

54 Wang, T., Sun, Z., Huang, D. et al. (2017). Studies on NH_3 gas sensing by zinc oxide nanowire-reduced graphene oxide nanocomposites. *Sens. Actuators, B* 252: 284–294.

55 Fang, W., Yang, Y., Yu, H. et al. (2017). An In_2O_3 nanorod-decorated reduced graphene oxide composite as a high-response NOx gas sensor at room temperature. *New J. Chem.* 41: 7517–7523.

56 Reddeppa, M., Park, B.-G., Kim, M.-D. et al. (2018). H_2, H_2S gas sensing properties of rGO/GaN nanorods at room temperature: effect of UV illumination. *Sens. Actuators, B* 264: 353–362.

57 Amarnath, M. and Gurunathan, K. (2021). Selective ammonia sensing response of vanadium doped cerium oxide nanorods wrapped reduced graphene oxide electrodes at room temperature. *Sens. Actuators, B* 336: 129679.

58 Kumar, R.R., Murugesan, T., Dash, A. et al. (2021). Ultrasensitive and light-activated NO_2 gas sensor based on networked MoS_2/ZnO nanohybrid with adsorption/desorption kinetics study. *Appl. Surf. Sci.* 536: 147933.

59 Viet, N.N., Dang, T.K., Phuoc, P.H. et al. (2021). MoS_2 nanosheets-decorated SnO_2 nanofibers for enhanced SO_2 gas sensing performance and classification of CO, NH_3 and H_2 gases. *Anal. Chim. Acta* 1167: 338576.

60 Liu, A., Lv, S., Jiang, L. et al. (2021). The gas sensor utilizing polyaniline/MoS_2 nanosheets/SnO_2 nanotubes for the room temperature detection of ammonia. *Sens. Actuators, B* 332: 129444.

61 Bai, X., Lv, H., Liu, Z. et al. (2021). Thin-layered MoS_2 nanoflakes vertically grown on SnO_2 nanotubes as highly effective room-temperature NO_2 gas sensor. *J. Hazard. Mater.* 416: 125830.

62 Zhang, D., Jiang, C., Li, P., and Sun, Y.e. (2017). Layer-by-layer self-assembly of Co_3O_4 nanorod-decorated MoS_2 nanosheet-based nanocomposite toward high-performance ammonia detection. *ACS Appl. Mater. Interfaces* 9: 6462–6471.

63 Zhao, S., Wang, G., Liao, J. et al. (2018). Vertically aligned MoS_2/ZnO nanowires nanostructures with highly enhanced NO_2 sensing activities. *Appl. Surf. Sci.* 456: 808–816.

64 Zhao, P., Tang, Y., Mao, J. et al. (2016). One-dimensional MoS_2-decorated TiO_2 nanotube gas sensors for efficient alcohol sensing. *J. Alloys Compd.* 674: 252–258.

65 Zhao, S., Li, Z., Wang, G. et al. (2018). Highly enhanced response of MoS_2/porous silicon nanowire heterojunctions to NO_2 at room temperature. *RSC Adv.* 8: 11070–11077.

66 Dwiputra, M.A., Fadhila, F., Imawan, C., and Fauzia, V. (2020). The enhanced performance of capacitive-type humidity sensors based on ZnO nanorods/WS_2 nanosheets heterostructure. *Sens. Actuators, B* 310: 127810.

67 Suh, J.M., Kwon, K.C., Lee, T.H. et al. (2021). Edge-exposed WS_2 on 1D nanostructures for highly selective NO_2 sensor at room temperature. *Sens. Actuators, B* 333: 129566.

68 Wang, B., Zheng, Z.Q., Zhu, L.F. et al. (2014). Self-assembled and Pd decorated Zn_2SnO_4/ZnO wire-sheet shape nano-heterostructures networks hydrogen gas sensors. *Sens. Actuators, B* 195: 549–561.

69 Liu, F., Chen, X., Wang, X. et al. (2019). Fabrication of 1D Zn_2SnO_4 nanowire and 2D ZnO nanosheet hybrid hierarchical structures for use in triethylamine gas sensors. *Sens. Actuators, B* 291: 155–163.

70 Wang, X. and Cho, H.J. (2018). p-CuO nanowire/n-ZnO nanosheet heterojunction-based near-UV sensor fabricated by electroplating and thermal oxidation process. *Mater. Lett.* 223: 170–173.

71 Lu, Y., Ma, Y., Ma, S., and Yan, S. (2017). Hierarchical heterostructure of porous NiO nanosheets on flower-like ZnO assembled by hexagonal nanorods for high-performance gas sensor. *Ceram. Int.* 43: 7508–7515.

72 Hoa, L.T., Tien, H.N., and Hur, S.H. (2014). Fabrication of novel 2D NiO nanosheet branched on 1D-ZnO nanorod arrays for gas sensor application. *J. Nanomater.* 2014.

73 Nakate, U.T., Yu, Y., and Park, S. (2021). High performance acetaldehyde gas sensor based on pn heterojunction interface of NiO nanosheets and WO_3 nanorods. *Sens. Actuators, B* 130264.

74 Wang, Z., Zhi, M., Xu, M. et al. (2021). Ultrasensitive NO_2 gas sensor based on Sb-doped SnO_2 covered ZnO nano-heterojunction. *J. Mater. Sci.* 56: 7348–7356.

75 Wang, B., Wang, Y., Lei, Y. et al. (2016). Vertical SnO_2 nanosheet@ SiC nanofibers with hierarchical architecture for high-performance gas sensors. *J. Mater. Chem. C* 4: 295–304.

76 Sun, L., Wang, B., and Wang, Y. (2020). High-temperature gas sensor based on novel Pt single atoms@ SnO_2 nanorods@ SiC nanosheets multi-heterojunctions. *ACS Appl. Mater. Interfaces* 12: 21808–21817.

77 Xu, K., Wei, W., Sun, Y. et al. (2019). Design of $NiCO_2O_4$ porous nanosheets/α-MoO_3 nanorods heterostructures for ppb-level ethanol detection. *Powder Technol.* 345: 633–642.

78 Xu, K., Zhao, W., Yu, X. et al. (2020). Enhanced ethanol sensing performance using Co_3O_4-$ZnSnO_3$ arrays prepared on alumina substrates. *Phys. E* 117: 113825.

79 Xu, K., Tang, Q., Zhao, W. et al. (2020). In situ growth of Co_3O_4@ $NiMoO_4$ composite arrays on alumina substrate with improved triethylamine sensing performance. *Sens. Actuators, B* 302: 127154.

80 Wang, Y., Zhou, Y., Ren, H. et al. (2020). Room-temperature and humidity-resistant trace nitrogen dioxide sensing of few-layer black phosphorus nanosheet by incorporating zinc oxide nanowire. *Anal. Chem.* 92: 11007–11017.

81 Wang, Y., Cao, J., Qin, C. et al. (2017). Synthesis and enhanced ethanol gas sensing properties of the g-C_3N_4 nanosheets-decorated tin oxide flower-like nanorods composite. *Nanomaterials* 7: 285.

82 Kim, J.-H., Mirzaei, A., Zheng, Y. et al. (2019). Enhancement of H_2S sensing performance of p-CuO nanofibers by loading p-reduced graphene oxide nanosheets. *Sens. Actuators, B* 281: 453–461.

83 Abideen, Z.U., Katoch, A., Kim, J.-H. et al. (2015). Excellent gas detection of ZnO nanofibers by loading with reduced graphene oxide nanosheets. *Sens. Actuators, B* 221: 1499–1507.

84 Chaudhary, V. and Nehra, S.P. (2021). Pt-sensitized MoO_3/mpg-CN mesoporous nanohybrid: a highly sensitive VOC sensor. *Microporous Mesoporous Mater.* 315: 110906.

85 Wang, L., Fu, H., Jin, Q. et al. (2019). Directly transforming SnS_2 nanosheets to hierarchical SnO_2 nanotubes: towards sensitive and selective sensing of acetone at relatively low operating temperatures. *Sens. Actuators, B* 292: 148–155.

86 Li, X., Zhou, Y., Tai, H. et al. (2020). Nanocomposite films of p-type MoS_2 nanosheets/n-type ZnO nanowires: sensitive and low-temperature ppb-level NO_2 detection. *Mater. Lett.* 262: 127148.

87 Hsu, L.C., Ativanichayaphong, T., Cao, H. et al. (2007). Evaluation of commercial metal-oxide based NO_2 sensors. *Sens. Rev.*

88 Kwak, C.-H., Kim, T.-H., Jeong, S.-Y. et al. (2018). Humidity-independent oxide semiconductor chemiresistors using terbium-doped SnO_2 yolk–shell spheres for real-time breath analysis. *ACS Appl. Mater. Interfaces* 10: 18886–18894.

89 Qu, F., Zhang, S., Huang, C. et al. (2021). Surface functionalized sensors for humidity-independent gas detection. *Angew. Chem., Int. Ed.* 60: 6561–6566.

90 Kondalkar, V.V., Duy, L.T., Seo, H., and Lee, K. (2019). Nanohybrids of Pt-functionalized Al_2O_3/ZnO core–shell nanorods for high-performance MEMS-based acetylene gas sensor. *ACS Appl. Mater. Interfaces* 11: 25891–25900.

91 Sajjad, M. and Feng, P. (2014). Study the gas sensing properties of boron nitride nanosheets. *Mater. Res. Bull.* 49: 35–38.

92 Ma, J., Fan, H., Zhang, W. et al. (2020). High sensitivity and ultra-low detection limit of chlorine gas sensor based on In_2O_3 nanosheets by a simple template method. *Sens. Actuators, B* 305: 127456.

93 Raghu, A.V., Karuppanan, K.K., Nampoothiri, J., and Pullithadathil, B. (2019). Wearable, flexible ethanol gas sensor based on TiO_2 nanoparticles-grafted 2D-titanium carbide nanosheets. *ACS Appl. Nano Mater.* 2: 1152–1163.

94 Deng, S., Liu, X., Chen, N. et al. (2016). A highly sensitive VOC gas sensor using p-type mesoporous Co_3O_4 nanosheets prepared by a facile chemical coprecipitation method. *Sens. Actuators, B* 233: 615–623.

95 Zhang, L., Li, Z., Liu, J. et al. (2020). Optoelectronic gas sensor based on few-layered InSe nanosheets for NO_2 detection with ultrahigh antihumidity ability. *Anal. Chem.* 92: 11277–11287.

96 Patel, L., Shukla, T., Huang, X. et al. (2020). Machine learning methods in drug discovery. *Molecules* 25: 5277.

97 Karthik, S. and Sudha, M. (2018). A survey on machine learning approaches in gene expression classification in modelling computational diagnostic system for complex diseases. *Int. J. Eng. Technol.* 8: 182–191.

98 Zhang, Y., Wong, Y.S., Deng, J. et al. (2016). Machine learning algorithms for mode-of-action classification in toxicity assessment. *BioData Min.* 9: 1–21.

99 Acharyya, S., Jana, B., Nag, S. et al. (2020). Single resistive sensor for selective detection of multiple VOCs employing SnO_2 hollowspheres and machine learning algorithm: a proof of concept. *Sens. Actuators, B* 321: 128484.

100 Jaeschke, C., Glöckler, J., El Azizi, O. et al. (2019). An innovative modular eNose system based on a unique combination of analog and digital metal oxide sensors. *ACS Sens.* 4: 2277–2281.

101 Peng, G., Tisch, U., Adams, O. et al. (2009). Diagnosing lung cancer in exhaled breath using gold nanoparticles. *Nat. Nanotechnol.* 4: 669–673.

102 Liao, Y.-H., Shih, C.-H., Abbod, M.F. et al. (2020). Development of an E-nose system using machine learning methods to predict ventilator-associated pneumonia. *Microsyst. Technol.* 1-11.

103 Salhi, L., Silverston, T., Yamazaki, T., and Miyoshi, T. (2019). Early detection system for gas leakage and fire in smart home using machine learning. In: *2019 IEEE International Conference on Consumer Electronics (ICCE)*, 1–6. IEEE.

104 Yaqoob, U. and Younis, M.I. (2021). Chemical gas sensors: recent developments, challenges, and the potential of machine learning-a review. *Sensor* 21: 2877.

105 Lekha, S. and Suchetha, M. (2020). Recent advancements and future prospects on E-Nose sensors technology and machine learning approaches for non-invasive diabetes diagnosis: a review. *IEEE Rev. Biomed. Eng.* 14: 127–138.